Dual copper- and photoredox-catalysed reactions

Tetrahedron
journal homepage: www.elsevier.com

Dual copper- and photoredox-catalysed reactions

Euan B. McLean[a] and Ai-Lan Lee[a,] *

[a]*Institute of Chemical Sciences, School of Engineering and Physical Sciences, Heriot-Watt University, Edinburgh EH14 4AS, Scotland, United Kingdom.*

ARTICLE INFO

Article history:
Received
Received in revised form
Accepted
Available online

Keywords:
Photoredox
Copper
Catalysis
Dual catalysis
Photocatalysis

ABSTRACT

The merger of transition metal catalysis with visible light photoredox catalysis in a cooperative fashion has recently emerged as a versatile way of developing new synthetic methodologies. This review will focus on the relatively new but fast expanding area of dual copper- and photoredox-catalysis, detailing recent developments in the area.

1. Introduction

In recent years, the discipline of organic synthesis has shifted its focus to developing greener and more sustainable synthetic methodologies. One area that has been the subject of substantial interest is the use of photoredox catalysts to harness visible light and promote new modes of reactivity from substrates and catalysts.[1] One methodology which has revealed itself to be a powerful bond forming tool is the synergistic combination of photoredox catalysts and transition metal catalysts in dual catalytic systems.[1f,2] The majority of these systems are able to carry out their target transformations under mild reaction conditions. These dual systems also benefit from the large redox potentials of the photocatalysts, which allow for the oxidation state of the transition metal catalyst to be manipulated, thereby opening up new reactive pathways without the need for super stoichiometric amounts of oxidants or reductants.[1f,2]

Since its inception, the field of dual transition metal and photoredox catalysis has been dominated by protocols which use nickel as the transition metal catalyst, with elegant seminal contributions from the groups of Molander and MacMillan demonstrating the wide scope and synthetic utility of this class of reaction.[3] Despite the clear advantages of using dual nickel and photoredox catalysis, commonly used nickel catalysts for this class of reactions are toxic and carcinogenic,[4] and for this reason, finding alternatives with lower toxicity would be beneficial. One emerging alternative to the use of nickel complexes is to use cheap and relatively non-toxic copper salts in conjunction with photoredox catalysts. These copper salts are not only less toxic, but also benefit from being able to catalyse reactions as inorganic salts without the need for ligands. Dual copper- and photoredox-catalysed methodologies have been much less explored compared to their nickel counterparts, but early examples have shown that they hold much promise. Such examples include the seminal work of Sanford, who demonstrated the first example of a dual copper- and photoredox-catalysed cross-coupling.[5]

The focus of this review will be to document the development of *dual* copper- and photoredox-catalysed methodologies using visible light, whilst highlighting the various proposed mechanisms for these transformations, where available. Reactions have been grouped together by the bonds which are formed during the reaction. There are other distinct classes of catalytic reactions involving visible light and copper, such as Cu-catalysed cross-couplings under visible light where no exogenous photosensitizer is required[6] or where copper is used solely as the photocatalyst.[7] Since these examples are generally mechanistically distinct from dual copper- and photoredox-catalysed methodologies and have previously been reviewed,[8] they will not be covered here except in cases where the process is thought to occur *via* a dual-catalytic cycle.

2. C-C Bond Formation

2.1. Fluoroalkylations

Fluorine containing organic compounds have drawn considerable interest as a result of their applications in pharmaceuticals and agrochemicals.[9] In particular, trifluormethylations are synthetically useful as the CF_3 moiety is present in a number of biologically active molecules.[9] As stated

* Corresponding author. Tel.: +44-(0)131-4518030; e-mail: A.Lee@hw.ac.uk

previously, the first synthetic application of dual copper- and photoredox-catalysis was in the seminal work of Ye and Sanford.[5] Using a catalyst system comprising a simple Cu(I) salt and $Ru(bpy)_3Cl_2.6H_2O$ (bpy = 2,2'-bipyridine) as a photocatalyst, Ye and Sanford were able to develop a mild protocol for the trifluoromethylation and perfluoroalkylation of aryl boronic acids **1** (Scheme 1).

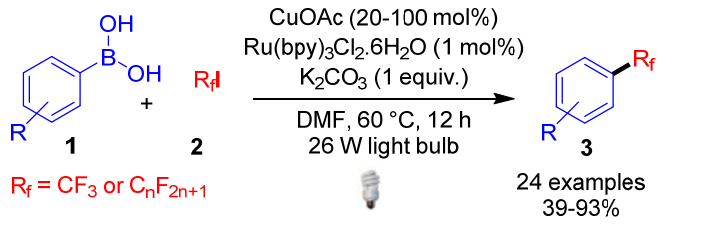

Scheme 1. Fluoroalkylation conditions developed by Ye and Sanford.[5]

Using readily available fluoroalkyliodides **2**, which form radicals under photoredox conditions, allowed for many of the limitations of previous methods to be circumvented, namely harsh conditions, expensive reagents and a narrow substrate scope.[10] In contrast, the conditions employed by Ye and Sanford tolerate a broad range of boronic acid substrates **1**, both electron-withdrawing (e.g. **3b**) and -donating substituents R (e.g. **3a**) were tolerated on the aryl ring, providing good to excellent yields of desired product **3** (64-93%, $R_f = CF_3$). All of these reactions were achieved using trifluoromethyl iodide as an inexpensive CF_3 source. Aryl boronic acids **1** that bear functional groups such as hydroxyl and carbonyl groups (e.g. **3c**), which have the potential to be highly reactive, also performed reasonably well (40-68%). The reaction is, however, sensitive to steric effects, with a noticeable drop in reaction performance for sterically demanding substrates such as mesityl and napthyl boronic acids (39 and 42% respectively). A range of heteroaromatic boronic acids could also be applied in the reactions with moderate success (48-67%, e.g. **3d**). This, coupled with the fact that a boronic acid derivative of estrone **1e** reacted to give **3e** in an 80% yield would suggest that this reaction could have potential applications in late stage modification of pharmaceuticals (Scheme 2).

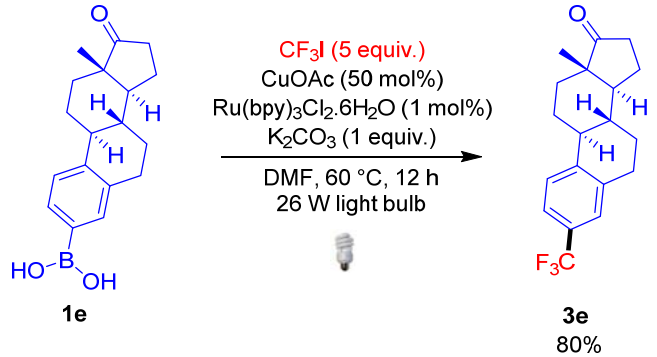

Scheme 2. Ye and Sandford's synthesis of trifluoromethylated estrone. [5]

A significant advantage of Sanford's method is that the scope of fluoroalkyliodides **2** can be expanded beyond trifluoromethyliodide to include longer alkyl chains, as long as higher copper loadings are employed (50-100 mol%). At 50 mol% Cu loading, a four carbon chain ($R_f = C_4F_9$) can be coupled to **1** (R= *para*-Ph) to give the product **3** in a 67% yield. Similarly, it was possible to couple a ten carbon chain ($R_f = C_{10}F_{21}$) using 1 equivalent of copper (71% of **3**). The reaction was demonstrated to be easily scalable and showed no appreciable lowering of yield when scaled up from 0.05 mmol to 5 mmol (76 and 70% respectively).

Although there are not yet any in depth mechanistic studies to probe the mechanism of this reaction, Ye and Sanford do propose a plausible mechanism based on experimental observation and thermodynamic data on redox potentials, as shown in Scheme 3. The proposed mechanism begins with visible light excitation of the ruthenium photocatalyst $Ru(bpy)^{2+}$ to $Ru(bpy)^{2+*}$, which by means of a single electron transfer, oxidises copper(I) complex **A** to copper(II) complex **B**. The ground state photocatalyst $Ru(bpy)_3^{2+}$ is then regenerated by reducing the fluoroalkyl iodide **2** through a second electron transfer, generating a perfluorinated alkyl radical **E** in the process. This radical **E** then attacks complex **B**, producing **C**, which subsequently undergoes a transmetallation with the boronic acid **1** to produce Cu(III) complex **D**. Reductive elimination of complex **D** then releases the alkylated product **3** and regenerates catalyst **A**. The authors state that the basis for this proposed mechanism is thermodynamic data, for example, the redox potentials of the species involved in the SETs allows the processes to be thermodynamically favoured. The authors also propose that the first step: oxidation of Cu(I) to Cu(II), generating the reduced photocatalyst $Ru(bpy)_3^{+}$, is implied by Cu(I) salts performing better in the reaction compared to Cu(II) salts, which cannot participate in this process. It should be noted that, in addition to the order of radical addition followed by transmetallation shown in Scheme 3, it is also feasible that transmetallation could occur on complex **B** which would then be followed by radical addition. With the mechanistic evidence available, it is not possible to rule out this second pathway.

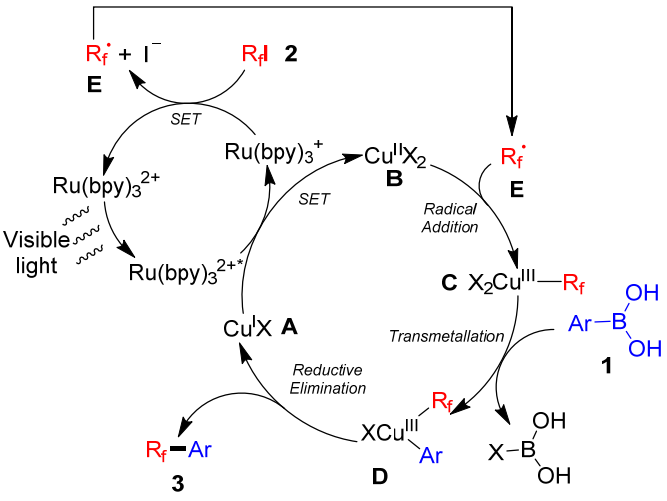

Scheme 3. Mechanism proposed by Ye and Sanford.[5]

It should be noted that in this reaction, as in many of the examples discussed in this review, the quantum yields have not been calculated. Radical chain mechanisms have since been shown to be of fundamental importance to photoredox catalysis, and quantum yield measurements are crucial to prove whether or not a radical chain mechanism is operating.[11] Therefore, in Scheme 3 as in all other proposed mechanisms where quantum yields were not measured, it should be noted that a radical chain mechanism cannot be ruled out.

Despite Ye and Sanford pioneering success, it was a number of years before the scope of dual copper- and photoredox-catalysed fluoroalkylations was expanded to include other substrates and radical sources. Further advancement in dual copper- and photoredox-catalysed fluoroalkylations came from group of Reiser in 2015.[12] This reaction by Reiser, is of a slightly different category as the cross-coupling is also catalysed by the same copper complex which acts as the photocatalyst *via* an inner-sphere co-ordination mechanism. In this work Reiser and co-workers developed a protocol for the dual copper- and photoredox-catalysed trifluoromethylchlorosulfonylation of alkenes **4** (Scheme 4).

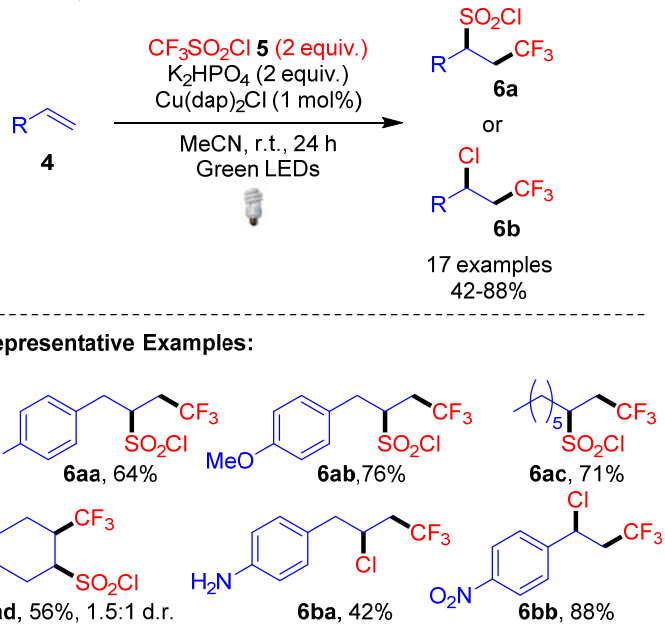

Scheme 4. Trifluoromethylchlorosulfonylation protocol developed by Reiser and co-workers.[12]

The use of Cu(dap)$_2$Cl (dap = 2,9-bis(*para*-ansyl)-1,10-phenanthroline) as photocatalyst allowed for the regioselective conversion of a range of terminal alkenes **4** to the corresponding trifluoromethylchlorosulfonylated product **6a** in moderate to excellent yields. In contrast, when the protocol is carried out using traditional ruthenium and iridium photocatalysts, the reaction proceeds with extrusion of SO_2 giving trifluoromethylchlorinated products **6b**. Under the conditions shown in Scheme **4**, allylbenzenes bearing both electron-withdrawing or electron-donating groups on the aromatic ring were transformed into the desired trifluoromethylchlorosulfonylated products (e.g. **6aa** and **6ab**) in good to excellent yields (64-87%). Both terminal alkenes with aliphatic side chains and cyclic internal alkenes are viable substrates and furnish the products (e.g. **6ac** and **6ad**) in moderate to good yields (56-78%). Interestingly, when the alkene substrate **4** contains a donor atom in close proximity to the alkene, product **6a** is not observed. Instead, only the trifluoromethylchlorinated products (e.g. **6ba**) are observed in moderate to good yields (42-64%). The authors report that styrenes can also undergo this trifluoromethylchlorination reaction, however, the products are prone to elimination reactions and are always observed as a mixture. The sole exception to this trend is when electron poor *para*-nitro styrene is used as a substrate: product **6bb** is isolated as the sole product in excellent yield (88%). The observed difference in the reaction outcome when Cu(dap)$_2$Cl is used as the photocatalyst compared to other more conventional photocatalysts led Reiser and co-workers to propose the mechanism in Scheme 5 to explain the difference in reactivity.

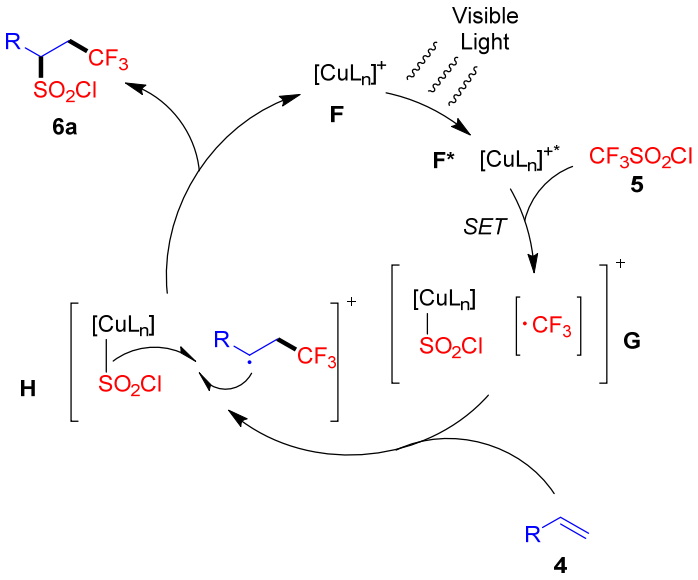

Scheme 5. Mechanism proposed by Reiser and co-workers.[12]

The authors propose that the transformation begins by photoexcitation of complex **F** to give excited state complex **F***. **F*** can then reduce **5** which simultaneously results in oxidation of Cu(I) to Cu(II) giving inner sphere species **G**. Attack of the trifluoromethyl radical from **G** gives intermediate **H**, from which the Cu(II) complex can deliver the SO_2Cl group to the alkyl radical, releasing product **6a** and regenerating photoactive complex **F**. The ability of the photoactive copper complex to play a dual role as both a photocatalyst and complexing agent for the reactive species in the reaction is key in allowing the chlorosulfonyl group to be included in the product **6a**. This is due to the inherent instability of the chlorosulfonyl anion which is known in literature to decompose very quickly releasing SO_2 and Cl^-.[13] Complexation to the copper catalyst stabilizes the chlorosulfonyl species allowing it to be installed in the final product **6a**. In contrast, the reaction with ruthenium and iridium photocatalysts most likely proceeds via an outer sphere mechanism which results in extrusion of SO_2 and chlorination of the final product **6b**. Formation of products such as **6ba** when there is a strong donor atom in the substrate **4** indicates the chlorosulfonyl group is only weakly bound to the copper catalyst and can be easily displaced. Varying the steric hindrance around the copper center was also shown to have a profound effect on whether the trifluoromethylchlorosulfonated product **6a** or the trifluoromethylchlorinated product **6b** is observed (Scheme 6). Changing the substrate from a monosubstitued alkene **4a** to only a slightly more hindered 1,1-disubstituted alkene **4b** results in a complete switch in selectivity, yielding product **6b** instead of **6a**. Additionally changing the Cu(dap)$_2$Cl photocatalyst for a catalyst where the co-ordination environment around the copper center is less sterically hindered (*i.e* Cu(dpp)(binc)Cl, binc = *bis*((*S*)-2-isocyano-3,3-dimethylbutyl)phenylphosphonate) results in a large increase in the ratio of **6af-6bd** (3:1 versus 9:1). Both of these pieces of evidence support the authors proposed inner sphere mechanism where the copper catalyst fulfills a dual catalytic role.

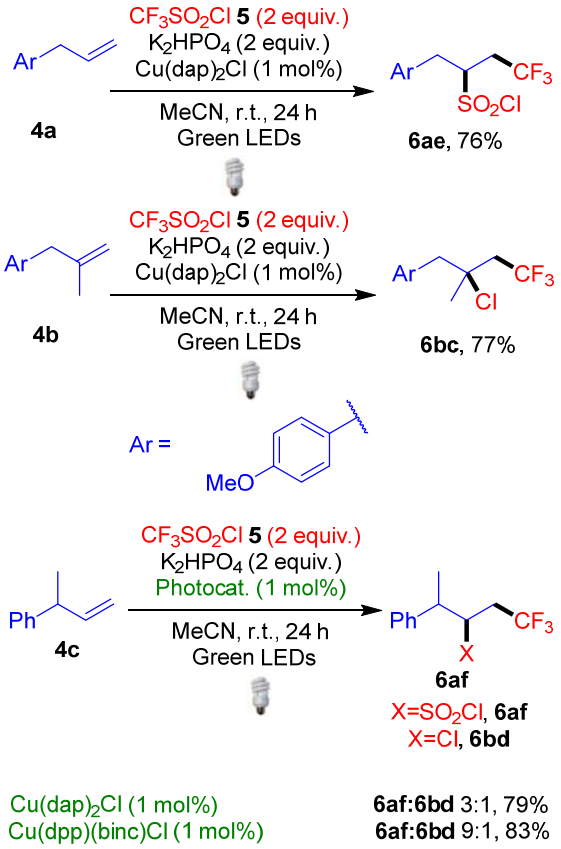

Scheme 6. Steric influence experiments carried out by Reiser and co-workers.[12]

Further evidence to support this mechanism come from the mixture of diasteromers produced for product **6ad** (Scheme 4) which indicates the participation of free CF_3 radicals, as the reaction would be expected to give the *cis*-addition product if the reaction was proceeding *via* $[CF_3CuSO_2Cl]^+$. The authors were also able to rule out the involvement of a radical chain mechanism due to the quantum yield of the transformation being measured to be 12%. In 2016, Reiser and co-workers expanded this work to the synthesis of trifluoromethylated sultones by including a tethered hydroxyl-nucleophile into the substrates.[14]

The next breakthrough came in 2016, when Qing and co-workers demonstrated that under dual copper- and photoredox-catalysed conditions, terminal alkenes **4** could undergo bromodifluoromethylation in the presence of (difluoromethyl)triphenylphosphonium bromide **7** to give **8** with excellent regioselectivity (Scheme 7).[15] The difluoromethyl (CF_2H) group is another structural motif that is currently undergoing an increasingly important role in drug discovery.[16]

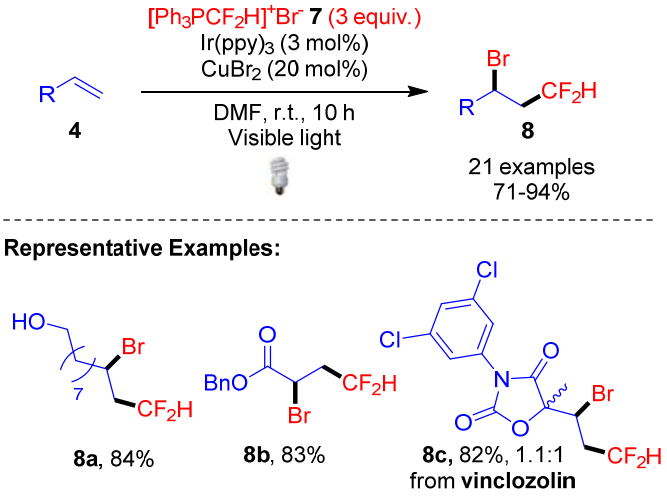

Scheme 7. Bromodifluoromethylation reported by Qing and co-workers.[15]

Although the photoredox reaction also proceeded in the absence of a copper catalyst, it was shown that catalytic amounts of $CuBr_2$ were crucial in almost totally suppressing the formation of hydrodifluoromethylated side products and thereby increasing the yield of desired product **8**. The reaction conditions used by Qing and co-workers also proved to be highly robust and tolerant of a number of diverse substrates. Alkene substrates containing a number of potentially highly reactive functional groups including alcohols, carbonyls and alkyl bromides were shown to be excellent substrates, providing the desired products **8** in excellent yields (81-94%, e.g. **8a**). Substrates bearing aryl halides **4** were also shown to be good substrates (71-88%), as were styrenes and *α,β*-unsaturated compounds (e.g. producing **8b**), which gave yields of 71% and 83% respectively. The potential of dual copper- and photoredox-catalysed reactions to be used in late stage modification was further emphasised when the authors demonstrated that the fungicide vinclozolin (see **8c**) and two insecticides allethrin and rotenone, were all viable substrates which could be bromodifluoromethylated in good yields (82%, 76% and 71% respectively). Qing and co-workers also demonstrated that difluoromethyl containing alkenes can be easily obtained from this methodology. Modifying the protocol to include a base promoted elimination step in a one-pot process provides access to difluoromethylated alkenes **9** in good yields with varying amounts of *E/Z* selectivity (Scheme 8).

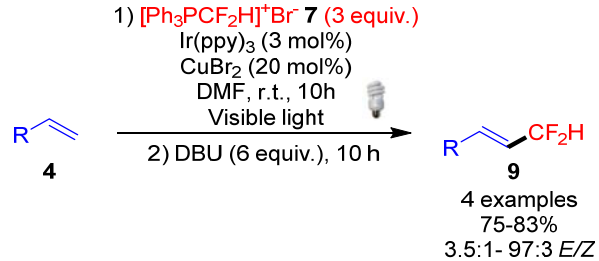

Scheme 8. One-pot bromodifluoroalkylation/elimination protocol developed by Qing and co-workers.[15]

Various experiments were undertaken in an attempt to elucidate the mechanism of the reaction. For example, under the reaction conditions, diene **4a** cyclises to give pyrrolidine derivative **10** (Scheme 9). This result suggests that the initial addition of CF_2H involves a CF_2H radical. In addition, no reaction is observed when (difluoromethyl)triphenylphosphonium bromide **7** is replaced with

difluoromethyl bromide (CF_2HBr), ruling the latter out as an intermediate in the mechanism. The reaction was also shown to take place with other triphenylphosphonium salts, such as (difluoromethyl)triphenylphosphonium triflate, provided that an additional source of bromide such as *n*-Bu_4NBr was included in the reaction mixture. Interestingly the chlorodifluoromethylated product could be obtained in a similar way using *n*-Bu_4NCl as the halogen source (63%); this result indicates that the halogen in the reaction adds in the form of the anion.

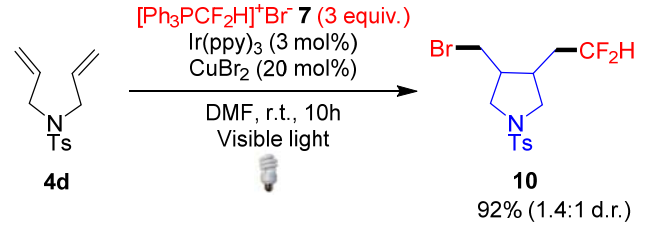

Scheme 9. Mechanistic experiment carried out by Qing and co-workers.[15]

Based on these studies, Qing and co-workers proposed possible mechanistic pathways for the reaction (Scheme 10). The proposed mechanism begins with excited state $Ir(ppy)_3^*$ (ppy = 2-phenylpyridyl) reducing (difluoromethyl)triphenylphosphonium bromide **7** *via* a single electron transfer to produce a bromide anion and a difluoromethyl radical. Addition of the radical into alkene **4** then gives radical intermediate **I**. From this point the authors propose that there are three plausible pathways, based on their mechanistic studies that lead to the desired product. Following pathway A, oxidation of **I** by $Ir(ppy)_3^+$ *via* a second single electron transfer produces cation **J** and regenerates the ground state photocatalyst. Nucleophilic attack of the bromide ion onto cation **J** then yields product **8**. Another possibility is that electron transfer from radical **I** to $CuBr_2$ gives cation **J**, which is then attacked by the bromide ion (pathway B). The third pathway proposed by Qing again involves reaction of radical **I** with $CuBr_2$. However, in this case the reaction produces alkyl copper species **K** which then goes on to react with the bromide ion to give the product **8**. The authors note that the exact role of the copper salt is not currently clear, so further study is required to elucidate the exact mechanism of the reaction.

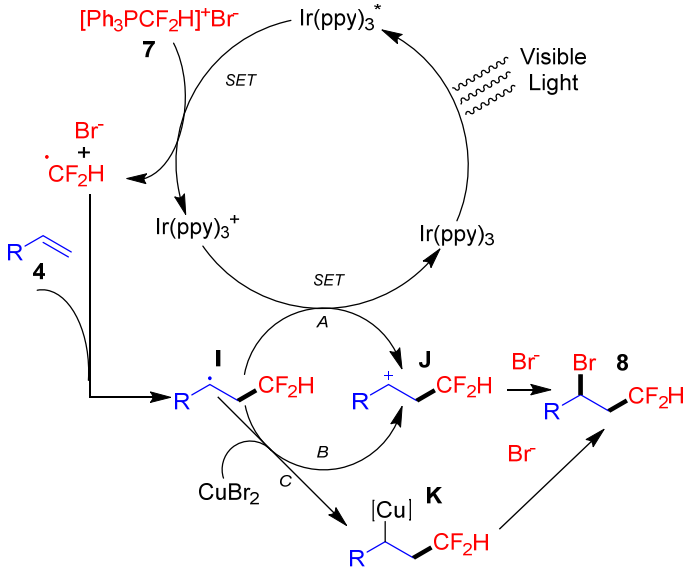

Scheme 10. Mechanistic pathways proposed by Qing and co-workers.[15]

Later in 2016, Liu and co-workers reported the decarboxylative difluoroacetylation of α,β-unsaturated carboxylic acids **11** under dual copper- and photoredox-catalysed conditions (Scheme 11).[17]

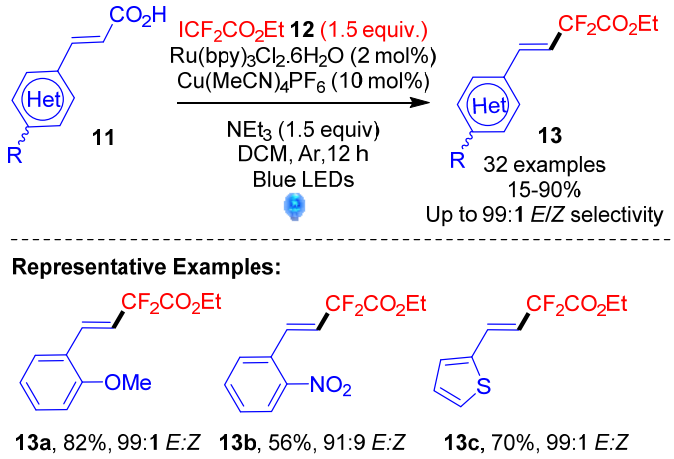

Scheme 11. Decarboxylative difluoroacetylation reported by Liu.[17]

The conditions shown in Scheme 11 were applied to a range of aryl-substituted α,β-unsaturated carboxylic acids **11** to give difluoroacetylated alkenes **13**, with varying yields and selectivities. Substrates **11** with electron-donating groups or halogens on the aryl ring performed well, furnishing the desired products (e.g. **13a**) in moderate to excellent yields (60-90%) and a high degree of *E*/*Z* selectivity in most cases (76:24 to 99:1 *E*/*Z*). In contrast, substrates **11** bearing strongly electron-withdrawing groups on the aromatic ring (such as a nitro group, e.g. **13b**) performed poorly, giving reduced yields (42-61%) and lower selectivities (58:42 to 91:9 *E*/*Z*). Liu and co-workers also go on to show that substrates **11** with heteroaromatic substituents, as opposed to aromatic substituents, are also compatible in the reaction (e.g. **13c**). Both electron-poor and electron-rich heteroaromatic substrates **11** give excellent selectivities (95:5 and 99:1 *E*/*Z* respectively). However electron-poor heterocycle substituents (e.g. 2-pyridine) on **11** result in very poor yields (15%) whereas electron-rich heterocycles (e.g. as 2-furan and 2-thiophene) perform considerably better (52%-70%).

In an attempt to gain some information on the mechanism, Liu and co-workers carried out the reaction in the presence of the well-known radical scavenger 2,2,6,6,-tetramethy-piperidinyloxy (TEMPO). In this experiment, formation of the desired product **13** was not observed, which led the authors to conclude that the mechanism most likely proceeds *via* a radical pathway. However, no TEMPO-radical adduct was isolated, so the identity of the radicals formed cannot yet be confirmed. Nevertheless, based on this evidence, Liu goes on to postulate a possible mechanism for this transformation, shown in Scheme 12.

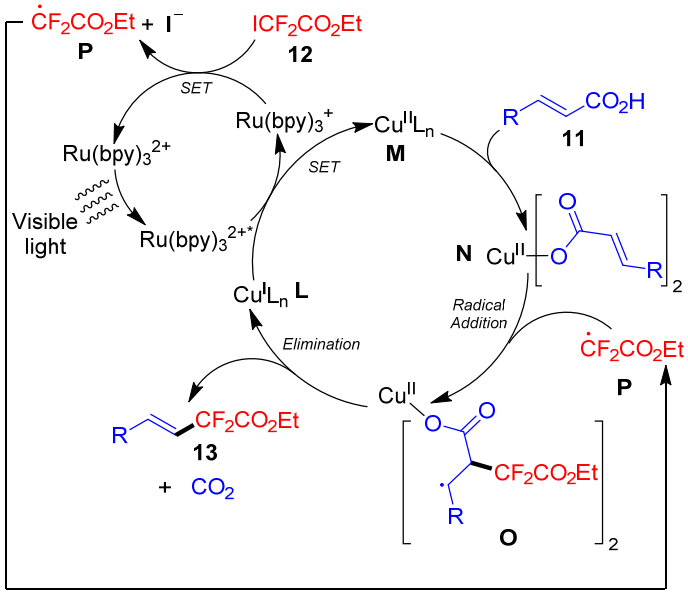

Scheme 12. Mechanism proposed by Liu.[17]

The authors propose that the first step in this mechanism is an oxidation of copper catalyst **L** by the excited state photocatalyst $Ru(bpy)_3^{2+*}$, generating copper(II) species **M** and $Ru(bpy)_3^{+}$. Co-ordination of substrate **11** to species **M** produces complex **N**. In complex **N**, the substrate is more activated towards radical attack from a CF_2CO_2Et radical **P** generated *via* reduction of ICF_2CO_2Et **12** by $Ru(bpy)_3^{+}$, which in the process regenerates the ground state photocatalyst $Ru(bpy)_3^{2+}$. This radical addition produces radical complex **O**, which through a decarboxylation process collapses to regenerate catalyst **L** while releasing product **13** and carbon dioxide. Nevertheless, more investigations will be required to determine whether or not this mechanism is operating.

2.2. Tetrahydroisoquinolines as Substrates

Tetrahydroisoquinolines **14** have attracted much attention in the context of substrates for dual copper- and photoredox-catalysis. This is most likely due to the ease at which tetrahydroisoquinolines undergo single electron oxidations.[18] There are a number of examples of dual copper- and photoredox-catalysed reactions of isoquinolines, all of which involve oxidation of the substrate **14** to the corresponding iminium cations followed by reaction with various nucleophiles. The first example of this type of reaction was reported by Rueping and co-workers in 2012.[19] In this work Rueping and co-workers successfully developed a protocol for the racemic *α*-*N*-alkynylation of tetrahydroisoquinolines **14** to yield **16** (Scheme 13).

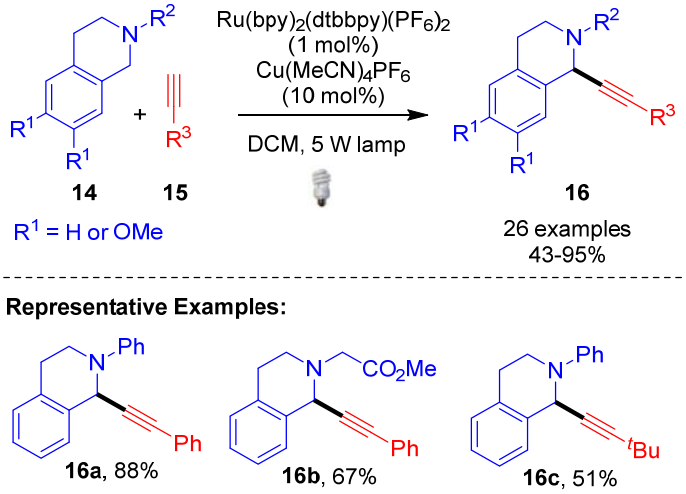

Scheme 13. Alkynylation protocol developed by Rueping and co-workers.[19]

In terms of the scope reported for this reaction, aryl substituents and glycine derivatives were investigated successfully (on R^2 in **14**, e.g. **16a** and **16b**). A range of substituents were reported for R^3, with aryl, alkyl, silyl and ester substituents on the terminal alkyne **15**. All of the substrates tested gave moderate to excellent yields of **16** (43-95%, e.g. **16c**). The only exception was when *p*-^{t}Buphenyl acetylene was used with a copper catalyst, however, replacing copper with a silver salt (AgO_2CCF_3) allows the reaction to proceed in a 77% yield. Although Rueping and co-workers do not propose a detailed mechanism for this transformation, they do suggest that it goes *via* an iminium ion intermediate generated by photoredox oxidation, which is then trapped by a copper catalysed addition of the alkyne.

In 2015, Li and co-workers built upon the early work of Rueping by developing an asymmetric dual copper- and photoredox-catalysed coupling of alkynes **15** and tetrahydroisoquinolines **17** using QUINAP ligand **18** (Scheme 14).[20]

Key differences between the protocols developed by Rueping and Li include: Rueping's reaction, shown in Scheme 13, benefits from the copper catalyst not requiring ligand stabilisation, however, addition of a chiral ligand is necessary in Li's reaction as this acts as the source of chiral induction. Furthermore, the enantioselective protocol requires much lower temperatures (-20 °C) for good enantioselectivities. Both aromatic and aliphatic alkynes **15** are compatible with the reaction and generally perform well, giving moderate to excellent yields (20-90%) of **19** with good enantioselectivities (80-94% e.e.). Aromatic alkynes **15** generally provide better yields and enantioselectivities than aliphatic alkynes (e.g. **19a** *vs.* **19b**). Despite giving a much lower yield (40%) and enantiomeric excess (60% e.e.) than many of the substrates studied, the reaction with trimethylsilyl (TMS) acetylene (**19c**) constitutes an improvement upon previous protocols based on non-photoredox methods (11% yield, 30% e.e.).[21] Most of the *N*-aryl tetrahydroisoquinolines **17** investigated in Li's work were compatible with the reaction, although there are some notable exceptions. The first exception is that the presence of bromine substituents on the aryl ring in **17** (R^1, Scheme 14) results in a dramatic drop in yield (20-30%) when reacted with **15** (R^2 = *n*-Bu or 4-$MeOC_6H_4$). However, good enantioselectivity is maintained (81-87% e.e.). Secondly, a substrate bearing a methoxy group in the 2-position of the aromatic ring on **17** proved to be prone to decomposition in reactions with **15** (where R^2 = Ph) under the standard conditions shown in Scheme 14. This was due to the

substrate being incompatible with the benzoyl peroxide oxidant. However, switching the terminal oxidant to molecular oxygen resulted in formation of the desired product **19** (80% yield, 80% e.e.).

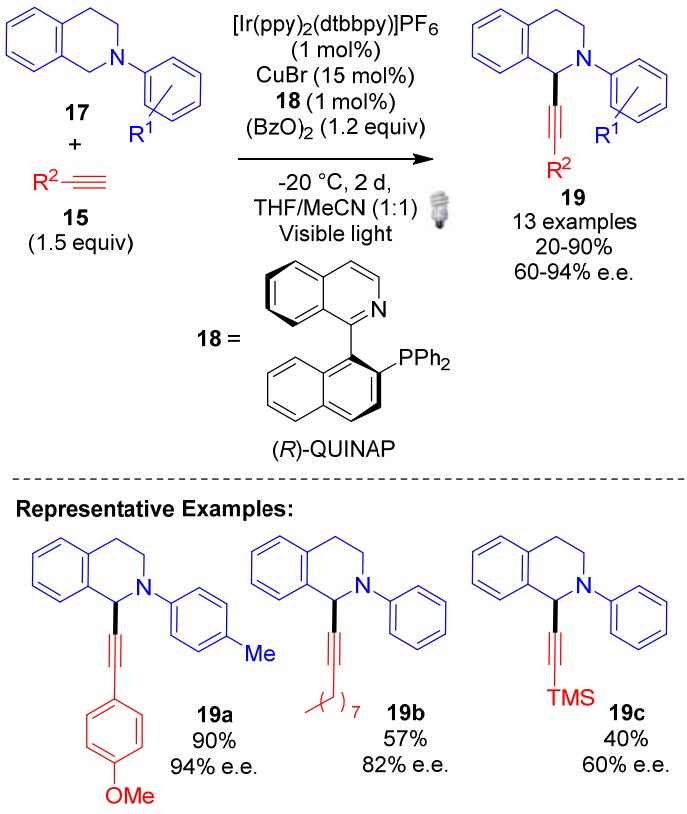

Scheme 14. Asymmetric alkynylation protocol developed by Li and co-workers.[20]

Li and co-workers propose a mechanism based on previous studies of the photcatalyst and cross dehydrogenative coupling reactions (Scheme 15).[19,21] Li's proposed mechanism begins with oxidation of tetrahydroisoquinoline **17** by the excited state Ir photocatalyst $Ir(ppy)_2(dtbbpy)^{+*}$ (dtbbpy = 4,4'-di-tert-butyl-2,2'-bipyridyl), forming radical cation **S**. The ground state photocatalyst $Ir(ppy)_2(dtbbpy)^{+}$ is then regenerated by single electron transfer from the reduced catalyst $Ir(ppy)_2(dtbbpy)$ to benzoyl peroxide, which generates an oxy-benzoyl radical **T** in the process. The oxybenzoyl radical **T** then abstracts the α-H from radical cation **S**, forming iminium ion **U**. Meanwhile, interaction of CuBr and chiral ligand **18** forms complex **Q**, which then reacts with alkyne **15** to form chiral copper acetylide **R**. Nucleophilic attack of **U** by copper acetylide **R** then forms product **19** and regenerates copper catalyst **Q**.

In the same year (2015), Duan and co-workers extended the utility of dual copper- and photoredox-catalysis from the homogenous to the heterogeneous domain.[22] In this work, the authors successfully demonstrated a new approach of merging Cu-catalysis and Ru-photocatalysis within a single metal organic framework (MOF). The MOF consisted of a Cu(II)-bipyridine structure with photoactive Ru containing $[SiW_{11}O_{39}Ru(H_2O)]^{5-}$ oxometallates contained in its pores. Duan co-workers demonstrated that this MOF is able to catalyse the addition of nitromethane and aryl ketones into *N*-phenyl tetrahydroisoquinoline **17** (Ar = Ph) in low to excellent conversions after 24 hours (10-90%). The authors propose that the copper centers in the MOF activate the nitromethane and aryl ketones as nucleophiles. These nucleophiles can then attack the iminium ions generated by photocatalytic oxidation of the tetrahydroisoquinoline substrates. The MOF showed a high degree of size specificity with a dramatic drop in yield when increasing the size of the aryl ketone substrates. This selectivity demonstrates that catalysis takes place within the MOF as opposed to on the surface to the MOF.

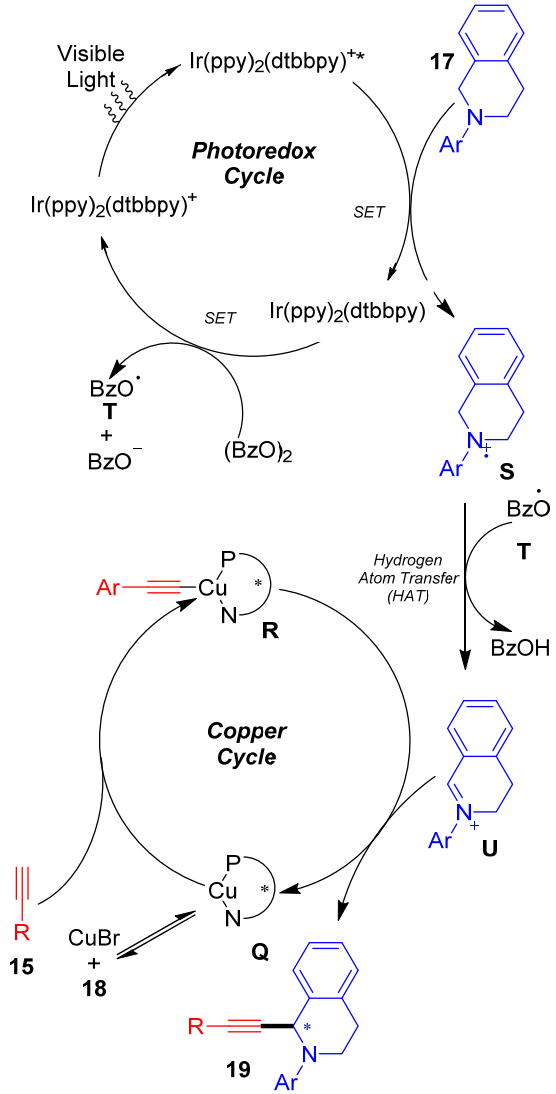

Scheme 15. Mechanism proposed by Li.[20]

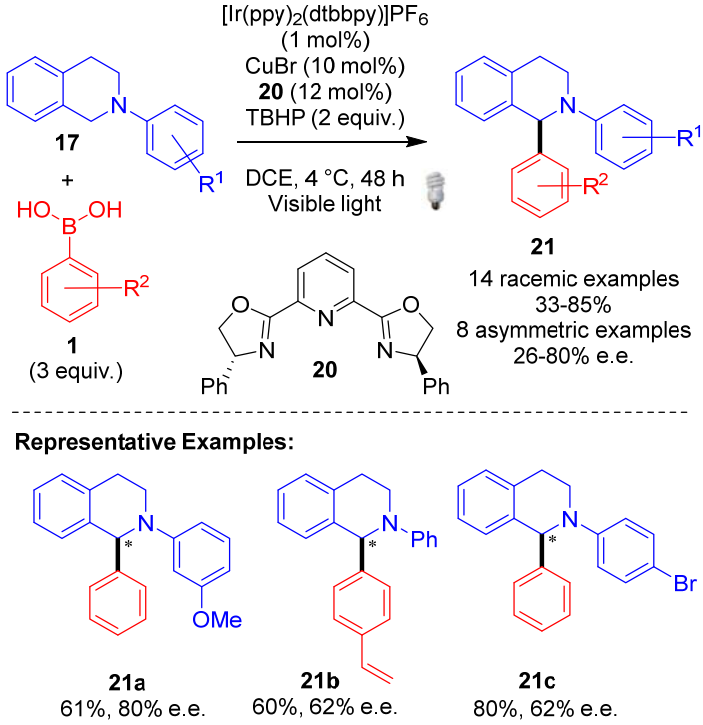

Scheme 16. Asymmetric arylation of tetrahydroisoquinolines reported by Li.[23]

In 2016, Li expanded the scope of asymmetric additions into tetrahydroisoquinolines **17** to include boronic acids **1** as nucleophiles (Scheme 16).[23] This work is closely related to their previous work on asymmetric additions of alkynes (Scheme 14), with similar catalytic systems employed.

The most notable change to allow the use of boronic acids **1** as nucleophiles is the change in chiral ligand from QUINAP ligand **18** to PhPyBox **20**. *N*-Aryls **17** bearing electron-donating R^1 groups perform well as substrates providing moderate to good yields of **21** (53%-78%). Substrates **17** with strongly electron-donating groups (R^1 = OMe) provide poorer yields than weak donors. The authors suggest that this is caused by substrates with strongly donating groups having lower oxidation potentials, which increases the probability of side reactions taking place. Mildly electron-withdrawing R^1 groups, such as halogens on the aromatic ring of tetrahydroisoquinolines **17** proved to be excellent substrates, furnishing the desired product **21c** in excellent yields (80% R^1 = Br, R^2 = H). Aryl boronic acids **1** with a range of electronic properties are tolerated as substrates, giving the desired products **21** in moderate to good yields (33-74%). As an overall trend, aryl boronic acids bearing electron-withdrawing groups gave lower yields and lower enantioselectivities. It was also demonstrated that the pyridyl moiety in the chiral ligand **20** was crucial for achieving high enantioselectivities, as replacing **20** with the corresponding PhBox ligand gave almost racemic product **21**.

The tentative mechanism proposed for this transformation is largely similar to the one that Li proposed for his previous related alkyne additions (Scheme 15). The one key difference is the change in proposed mode of delivery as the nucleophile changes from alkyne **15** to boronic acid **1**. In the previous work with acetylenes (Scheme 15), Li suggests that a copper acetylide **R** formed *in situ* acts as the nucleophile, delivering the alkyne to the iminium ion **U**. In contrast, when aryl boronic acids **1** are used as nucleophiles, Li postulates that the chiral copper complex co-ordinates to the π-bond of the iminium ion **U**, which activates it towards delivery of the aryl group from the boronic acid. Nevertheless, further mechanistic studies will be required to rule out other possibilities, such as transmetallation between copper and the aryl boronic acid **1**.

2.3. Other Substrates

In addition to the previously discussed classes of reactions, there have been a number of other C-C bond forming dual copper- and photoredox-catalysed reactions reported in the last couple of years. The first of these was reported by the group of Ackermann in 2016.[24] Although the main focus of Ackermann's publication is on copper catalysed C-H arylations induced by UV light, there is a single example showing that the C-H arylation can also be promoted by visible light in the presence of an iridium photocatalyst (Scheme 17). This dual copper- and photoredox-catalysed procedure allows for copper-catalysed C-H arylations of benzothiazoles **22** with aryl iodides **23** at mild temperatures. As the dual-catalysed reaction shown in Scheme 17 was a single proof-of-concept example and not the sole focus of the publication, there was no proposed mechanism for the transformation.

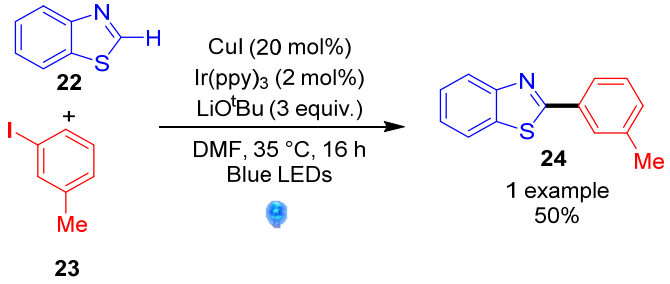

Scheme 17. Dual photoredox copper catalysed C-H arylation reaction reported by Ackermann.[24]

In 2017, Fu and co-workers developed a protocol for the decarboxylative alkynylation of *α*-amino acid derivatives **25** using dual copper- and photoredox-catalysis (Scheme 18).[25] In this protocol, amino acid derivatives **25** with alkyl side chains perform better than those with aryl side chains (83-95% *versus* 53-64%, e.g. **26a** *vs.* **26b**). Alkyl groups with varying steric bulk are all viable *N*-substituents providing **26** in yields that range from 70-95%. The reaction displays tolerance for a large range of functional groups on the alkyne coupling partner **15**. Alkynes with ethers, carbonyls, halogens and nitrogen containing substituents all perform well, furnishing the products **26** in good to excellent yields (60-95%, e.g. **26c**). In addition to the large substrate scope, Fu and co-workers demonstrated the synthetic utility of this transformation by carrying the reaction out on gram scale, providing the product **26d** in an excellent yield of (86%) with no significant drop in reaction performance when compared with the small scale result (89%) (Scheme 18).

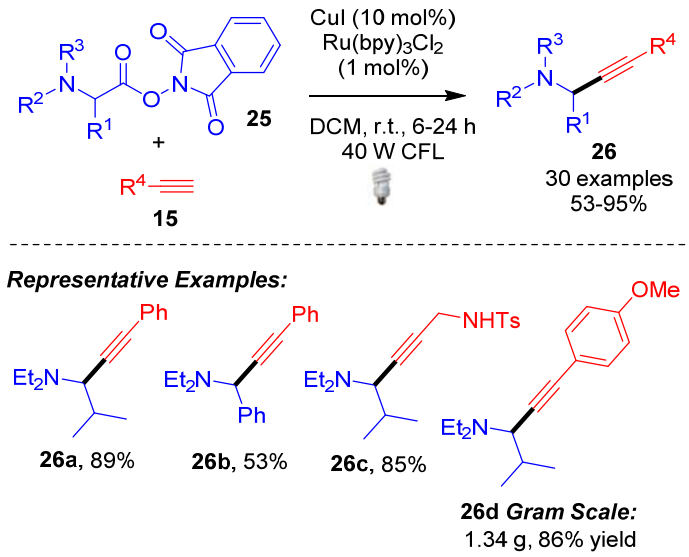

Scheme 18. Decarboxylative alkynylation developed by Fu.[25]

Fu's proposed mechanism begins with reduction of the excited state photocatalyst $Ru(bpy)_3^{2+*}$ *via* a single electron transfer from a molecule of starting material **25** (Scheme 19). The photocatalyst $Ru(bpy)_3^{+}$ is then a strong enough reductant to reduce another molecule of **25**, forming radical anion **W**. Radical anion **W** then decomposes to give radical **Y**, releasing a phthalimide anion **X** and carbon dioxide in the process. Radical **Y** is subsequently oxidised to iminium ion **Z** by the excited state photocatalyst $Ru(bpy)_3^{2+*}$ *via* a single electron transfer. Iminium **Z** is then intercepted by copper acetylide complex **AA** to give product **26**. The main experimental evidence for this mechanism comes from electron spin resonance (ESR) studies undertaken on the reaction. Irradiation of a solution comprising both catalysts, substrate **25** and radical trapping agent 5,5-dimethyl-1-pyrroline N-oxide (DMPO) and subsequent ESR analysis showed a quartet signal characteristic of a DMPO nitrogen radical adduct, which corresponds to radical **V**. Further investigation showed that when a similar solution was irradiated prior to addition of DMPO, three radical signals were observed. One signal was characteristic of an adduct formed between DMPO and a carbon radical, which again corresponds to radical **V**. The second was characteristic of a nitrogen-DMPO adduct and corresponds to radical **Y**. There was also a third signal which was not assigned by the authors but was reported to be a sextet which is characteristic of a carbon radical DMPO adduct. This evidence, combined with observations from previous research, forms the basis for the proposed mechanism shown in Scheme 19.[1m,26] Note, however, that the mechanism proposed in Scheme 19 remains putative until further mechanistic proof is established.

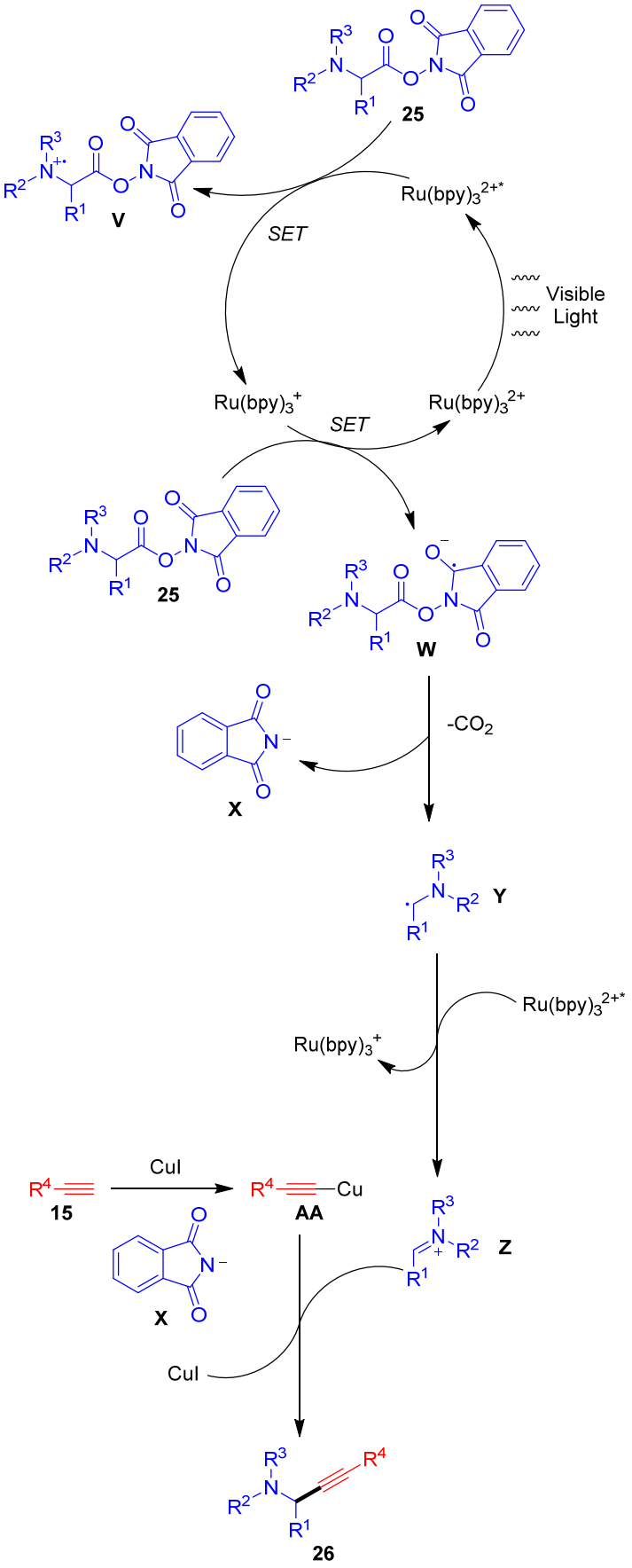

Scheme 19. Decarboxylative alkynylation mechanism proposed by Fu and co-workers.[25]

So far, this review has only included examples of intermolecular transformations. However, dual copper- and photoredox-catalysis can also be used for intramolecular cyclisations to form heterocycles. This is well demonstrated by the work of Xia and co-workers, who in 2017 developed three related protocols for the synthesis of quinolone derivatives with varying substitution patterns *via* oxidative cyclisations.[27] The first reaction involved an enamine-alkyne cyclisation shown in Scheme 20.

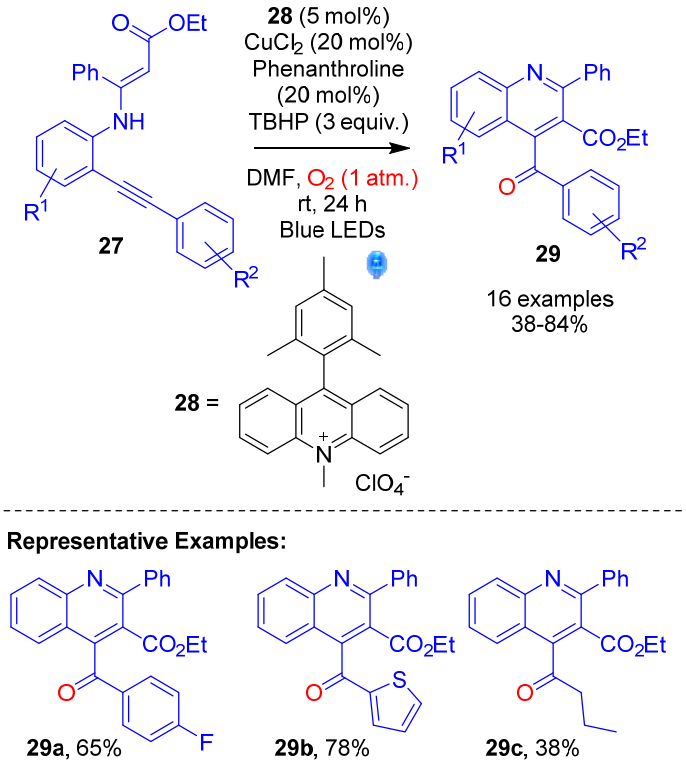

Scheme 20. Enamine-alkyne oxidative cyclisation devised by Xia and co-workers.[27]

This protocol has the advantage that it uses acridinium dye **28** (often known as Fukuzumi's catalyst, and shortened to Mes-Acr-Me$^+$)[28] as the photocatalyst, which is significantly cheaper than [Ru] and [Ir] photocatalysts. The scope of substituents on either ring is limited to either alkyls, halogens or no substituents, but all are well tolerated on both rings (58-84%, e.g. **29a**). Heteroaromatics can replace the R^2 aryl ring of **24** without any impact on reaction performance (**29b**, 78%). However when the same ring is replaced with an alkyl chain, the yield suffers considerably (**29c**, 38%). Interestingly, the authors note that the electron-withdrawing group (ester on **27**) seems vital for stabilising one of the radical intermediates. Substituting the ester group for a methyl or phenyl in substrate **27** results in only traces of the desired product **29** being formed. When 2 equivalents of TEMPO were added to the reaction mixture, only traces of the desired product **29** was detected. This could imply that the mechanism is radical based and TEMPO is inhibiting the reaction by trapping the radicals. However, no TEMPO-radical adduct was isolated during this experiment, therefore, other modes of inhibition such as catalyst deactivation cannot be ruled out. As an additional probe into the mechanism, Xia and co-workers carried out ^{18}O labelling experiments. Carrying the reaction out in an atmosphere of $^{18}O_2$ resulted in incorporation of ^{18}O into the ketone of product **29**. In addition, adding $H^{18}O_2$ to the standard reaction mixture resulted in no ^{18}O incorporation. These two pieces of evidence show that the carbonyl in product **29** is a result of aerobic oxidation by molecular oxygen. With this evidence in hand, Xia goes on to suggest a mechanism for the transformation (Scheme 21).

The mechanism begins with photocatalytic oxidation of substrate **27**, forming radical intermediate **AB** after loss of a proton. This radical then cyclises onto the alkyne to give intermediate **AC**, which subsequently undergoes a copper facilitated aerobic oxidation to give intermediate **AD**. This intermediate then collapses to give product **29** and releases the copper catalyst.

In addition to the already discussed transformation (Scheme 20), the work of Xia and co-workers also included two other oxidative intermolecular cyclisations. With slight alterations to the reaction conditions, substituted quinolone derivatives **32** and **35** could be obtained from substrates **30** and **33** as shown in Schemes 22-23. Both these modified protocols expand the number of substitution patterns tolerated by this methodology to generate the decorated quinolone scaffold. Furthermore, each of these reactions has a similar functional group tolerance with a number of reactive functionalities, most notably halogens being compatible with the transformation.

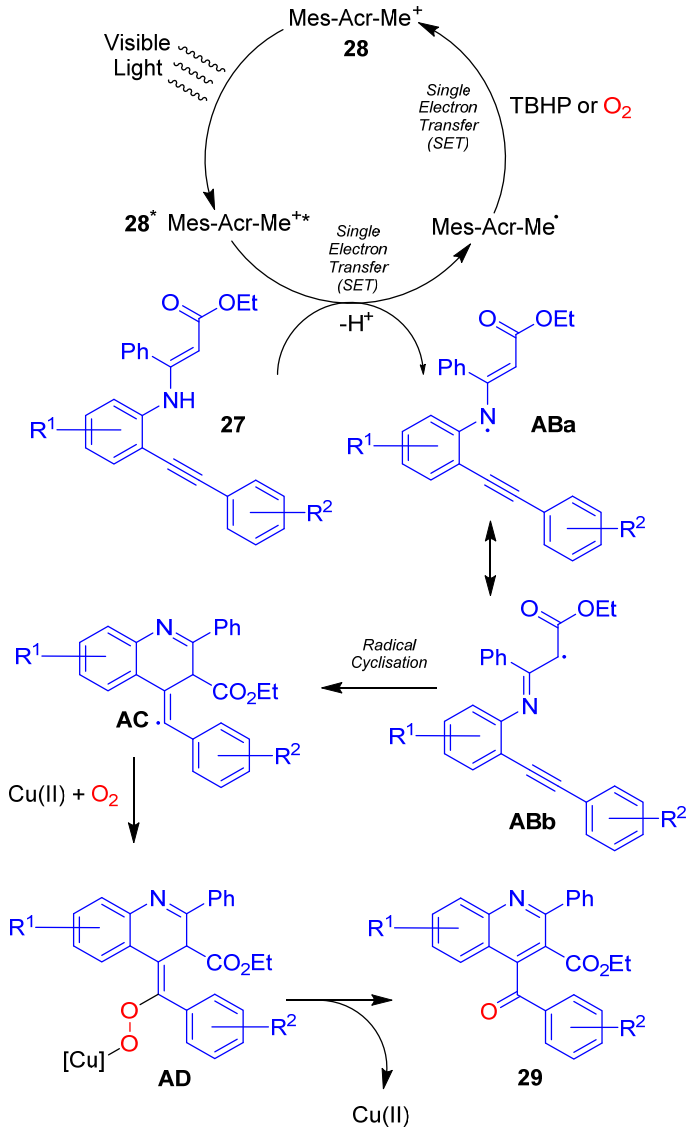

Scheme 21. Oxidative cyclisation mechanism proposed by Xia.[27]

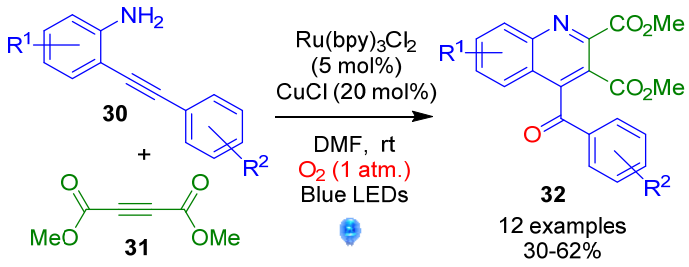

Scheme 22. Xia's first modified protocol.[27]

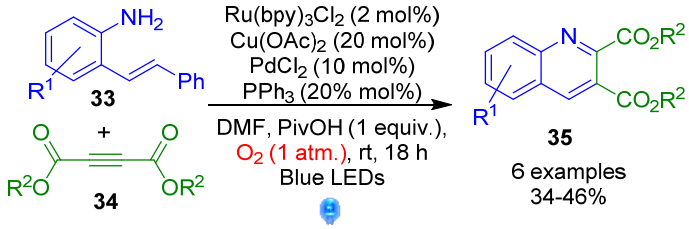

Scheme 23. Xia's second modified protocol.[27]

Dual copper- and photoredox-catalysed C-C bond forming reactions are not merely limited to cross-coupling reactions. This is perhaps best demonstrated by the work of Lin, Liu and co-workers in 2017.[29] In this work, the group developed a protocol for the asymmetric decarboxylative cyanation of *N*-hydroxy-phthalimide (NHP) esters **36** to yield **38** in good to excellent enantioselectivities (Scheme 24).

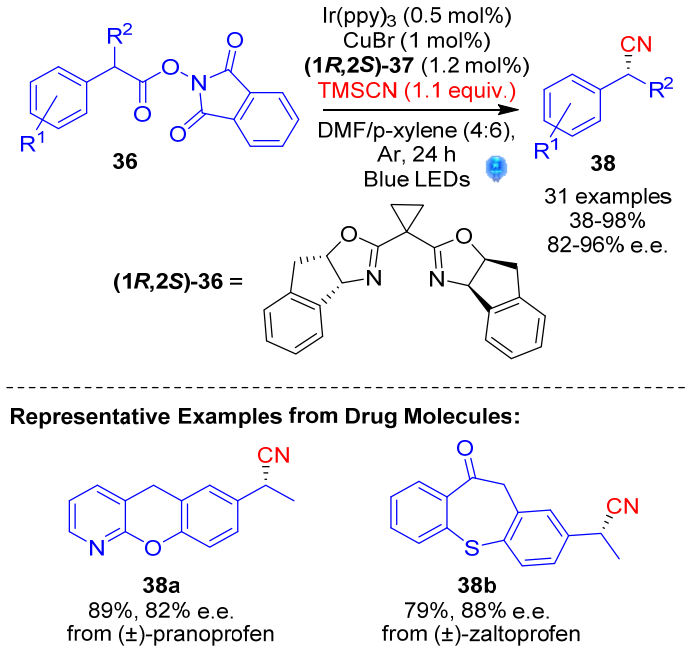

Scheme 24. Decarboxylative cyanation developed by Lin and Liu. [29]

This reaction has a wide scope of functional group tolerance: all reactions with substrates **36** based on simple carboxylic acid precursors furnished the products **38** in high yields (71%-91%) and high enantioselectivities (82%-99% e.e.). Sterically demanding substrates are well tolerated on the whole and the authors report that the added steric bulk actually enhances the enantioselectivity of the transformation. The reaction also tolerates a number of potentially reactive functional groups such as esters and halogens on R^1. The potential for dual copper- and photoredox-catalysis to be used in the pharmaceutical industry is further demonstrated by Lin and Liu as they use this protocol to functionalise a range of heterocycles and drug molecules such as pranoprofen and zaltoprofen (Scheme 24) in good yields and enantioselectivities (59%-98% and 82%-92% e.e. respectively). In addition, the reaction's synthetic utility is further increased by easy scale up to 0.27 mmol of **38** (R^1 = H, R^2 = Me) with no appreciable reduction in yields or enantioselectivity (34.3 g, 95% and 88% e.e. respectively). For practical ease, the authors also demonstrate that the parent carboxylic acids (e.g. **39**) can be used as substrates in a one-pot process, where they are converted to the NHP ester **36** *in situ* prior to the dual copper- and photoredox-catalysed cyanation (Scheme 25). Carrying the reaction out in this manner also has no negative impact on the yield or enantiomeric excess of **38c** (94%, 91% e.e.).

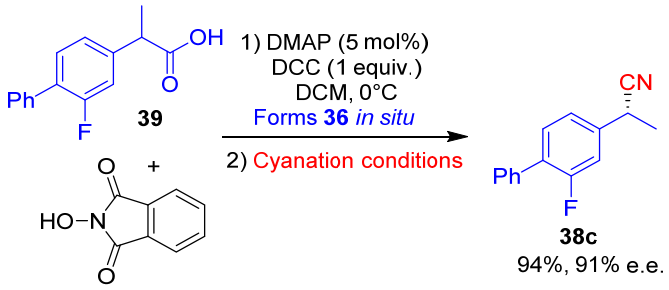

Scheme 25. One-pot cynanation protocol developed by Lin, Liu and co-workers. [29]

Although Lin and Liu do not propose a full catalytic cycle, the group undertook a series of mechanistic experiments to gain insight into the pathway by which this transformation is operating. The authors measured the reduction potential of a model NHP ester **36** to be -1.33 V in MeCN; the reduction of the ester by the excited state $Ir(ppy)_3$ photocatalyst ($E_{1/2}^{red}[Ir^{IV}/Ir^{III*}]$ = -1.73 V) should therefore be favoured.[30] Additionally, once oxidised, the photocatalyst $Ir(ppy)_3$ should have sufficient oxidative power ($E_{1/2}^{red}[Ir^{IV}/Ir^{III}]$ = +0.77 V) to oxidise a Cu(I)CN complex to Cu(II). The group measured the oxidation potential of this species to be $E_{1/2}^{red}[Cu^{II}/Cu^{I}]$ = +0.36 V. Further investigation showed that when TEMPO was included in the reaction mixture, the TEMPO adduct of the decarboxylated radical can be successfully isolated, indicating that the decarboxylation process is radical in nature. This finding was supported by subsequent radical clock experiments as well as the observation that enantiopure NHP esters **36** provide different enantiomers of product **38** depending on the configuration of the chiral ligand **37**. Finally Stern-Volmer fluorescence experiments showed that the excited state photocatalyst $Ir(ppy)_3^*$ is more likely to reduce the substrate **36** than interact with the copper catalyst, indicating that an oxidative quenching pathway is operating.

In 2016, Guo and co-workers reported on the merging of photoredox catalysis with copper Lewis acid catalysis in order to activate alkynes towards nucleophilic attack from weak nucleophiles (Scheme 26).[31] As shown in Scheme 26, the authors propose that the copper-activated 3c-2e alkyne complex **AE** is unreactive towards weak nucleophiles, however, SET oxidation *via* photoredox catalysis should produce a much more reactive $[Cu(II)\text{-alkyne}]^+$ complex **AF**, which would be susceptible towards attack by weak nucleophiles.

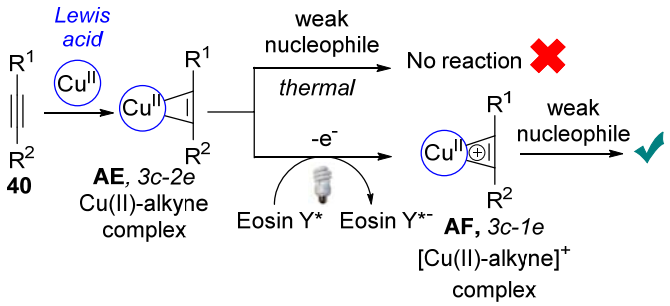

Scheme 26. Guo's proposed dual photoredox-catalysis with Lewis acid catalysis for activating carbon-carbon triple bonds.[31]

Based on their proposal shown in Scheme 26, a series of phenanthrenes **42** were successfully synthesized in good to excellent yields from arene-alkyne substrates **41** (83-100%, Scheme 27). In this case, the weak nucleophile is the aryl moiety, which does not react under thermal conditions, but successfully cyclizes under the dual catalytic conditions shown in Scheme 27. The organic dye Eosin Y is utilized as the photocatalyst, with $Cu(OTf)_2$ as the Lewis acid. A selection of both electron-donating as well as weakly electron-withdrawing groups are tolerated (R^1, R^2 and R^3 on **41**), but higher temperatures are required for the latter (e.g. 60 °C *vs.* RT for **42b** *vs.* **42a**). Although a 23 W household lamp was used for the substrate scope study, the use of a green LED lamp was found to accelerate the reaction (11 h vs. 4 h respectively for **42a**).

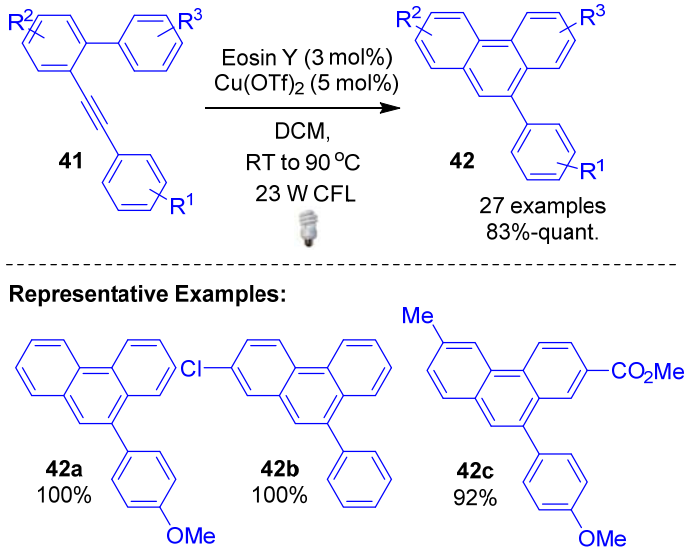

Scheme 27. Guo's dual photoredox-catalysis with Lewis acid catalysis for cyclisation of arene-ynes.[31]

Bode has recently shown the power of combining light induced reactions and Lewis acids to allow a distinct Ir(III)*/Ir(IV) couple (*vs.* previously employed Ir(III)*/Ir(II) pathways using photoredox catalysis alone), thereby enabling a wider range of transformations for the photocatalytic synthesis of *N*-heterocycles (e.g. **45)** from aldehydes and ketones using the silicon amine protocol (SLAP, Scheme 28).[32]

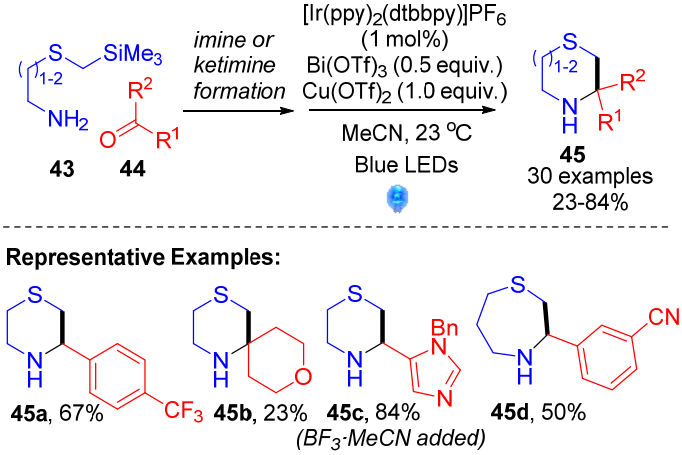

Scheme 28. Bode's dual photoredox-catalysis with Lewis acid catalysis for synthesis of *N*-heterocycles.[32]

During the optimization process, it was found that $Bi(OTf)_3$ as the Lewis acid performed better with certain aldehydes, while $Cu(OTf)_2$ worked better for others. As a result, a compromise of adopting *both* Lewis acids was used in the optimized general conditions. Thus, cyclized products **45** were formed in moderate to good yields with various aryl substituents (e.g. **45a**). Aliphatic, hindered and alkene substituents were also tolerated, albeit in modest yields (23-32%, e.g. **45b**). Seven-membered rings are also accessible in 43-50% yields (e.g. **45d**). A variety of heteroaromatic substituents were also successfully installed (e.g. **45c**), as long as the basic nitrogen atoms on the heteroaryls are protected *in situ* from binding to the Lewis acids $Bi(OTf)_3$ and $Cu(OTf)_2$, by adding N+1 equiv. of BF_3·MeCN.

As shown in Scheme 29, in the absence of a Lewis acid, a reductive quenching cycle operates (Scheme 29A), whereas the addition of a Lewis acid such as $Cu(OTf)_2$ switches the catalytic cycle to oxidative quenching (Scheme 29B). This switch allows for the photomediated synthesis of thiomorpholines and thiazepanes (**45**), which were not possible using photoredox catalysis alone. Mechanistic studies, including Stern-Volmer fluorescence quenching experiments led the authors to propose that Lewis acids activated imines **AE** serve as electron acceptors by reacting with photoexcited Ir(III)* to generate Ir(IV), thereby initiating the photocatalytic cycle. The resulting Ir(IV) possesses higher oxidation ability than Ir(III)* ($E_{1/2}^{IV/III} = +1.69$ V *vs* $E_{1/2}^{*III/II} = +0.66$ V) and is therefore able to promote SET oxidation on the sulfur atom of **AG** to give **AH**, and loss of $SiMe_3^+$ gives radical **AI**. After cyclization of **AI**, the resulting Lewis acid coordinated *N*-centered radical **AJ** has a lower reduction potential than its uncoordinated counterpart, which means that the catalytic cycle can be completed by reduction with Ir(III)*.

It should be noted that Wu and co-workers have also reported on a dual photoredox catalytic cycle involving $Cu(OTf)_2$ as a Lewis acid, for activating isochromans.[33] In this case, however, the main dual catalytic cycle involves cobalt and photoredox catalysis, and the reaction can still proceed in the absence of copper. Since the copper is only added to boost yields and is not necessary for the reaction to proceed, it is distinct from the dual-copper and photoredox-catalysed processes covered in this review.

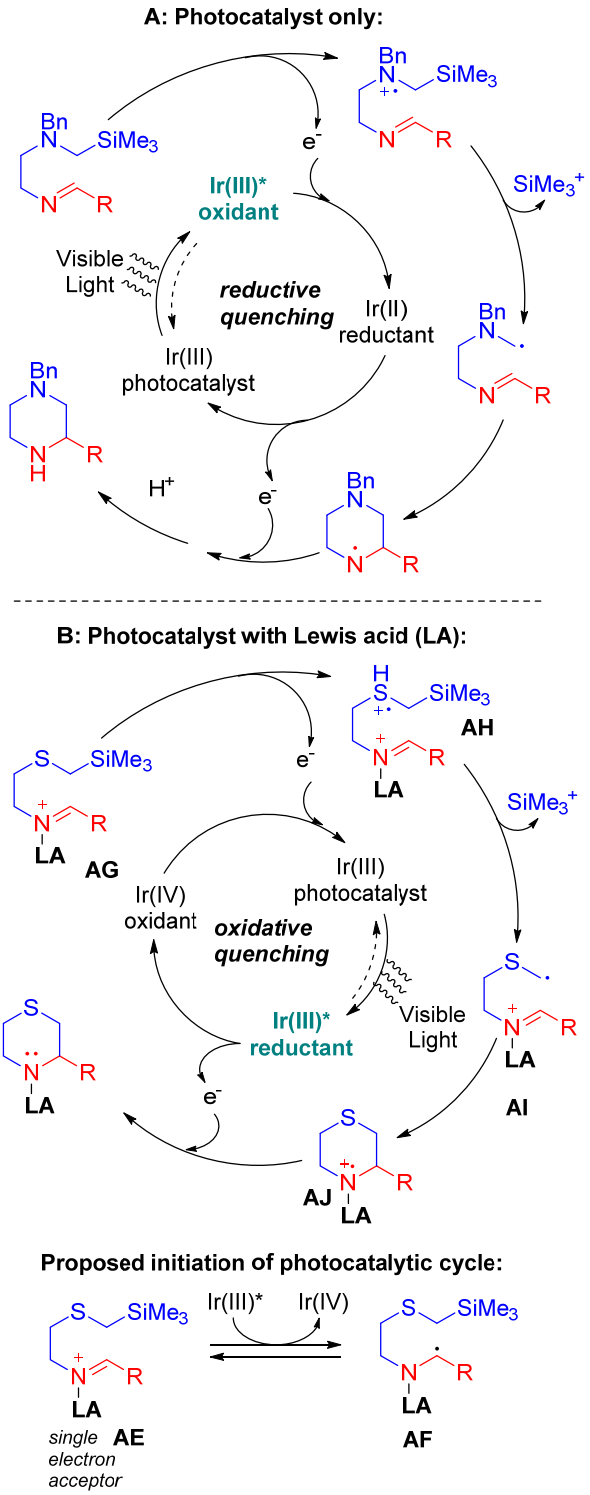

Scheme 29. Bode's proposed mechanistic switch in the presence of Lewis acids: photocatalyst only for piperazine synthesis and Lewis acid with photocatalyst for thiomorpholine/thiazepane synthesis.[32]

3. C-Heteroatom Bond Formation

3.1. C-N Bond Formation

In contrast to C-C bond forming reactions, it is only in recent years that dual copper- and photoredox-catalysis methodology has been applied to C-heteroatom bond forming reactions. The first example of such a transformation was reported in 2015 by the group of Kobayashi. In this pioneering work, they discuss the development of a photoredox-mediated Chan-Lam cross-coupling using aniline derivatives **46** and aryl boronic acids **1** (Scheme 30).[34]

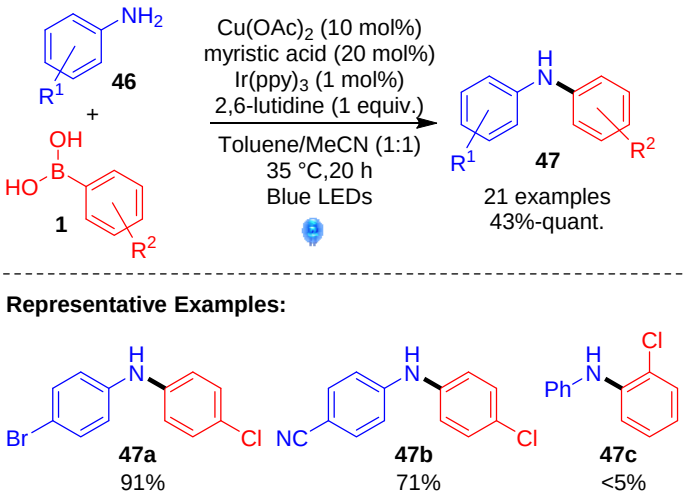

Scheme 30. Photoredox-mediated Chan-Lam coupling developed by Kobayashi and co-workers.[34]

Using arylboronic acid **1** R^2 = 4-Cl as a model, anilines **46** with slightly electron-donating substituents prove to be excellent substrates with yields ranging from 93% to quantitative yield. However, those with strongly electron-donating substituents perform poorly (43%); it is worth noting that this result is not dissimilar from the non–photoredox Chan-Lam result. Anilines with halogen substituents are also very good substrates, furnishing the coupled product **47** in very high yields (91-100%, e.g. **47a**, Scheme 30). Electron-poor anilines **46** are also tolerated with slightly reduced yields (42%-71%, e.g. **47b**, Scheme 30). Arylboronic acids with a range of electronic properties are all tolerated giving fair to excellent yields (R^1 = H) (43%-quant.). However, the reaction exhibits extreme sensitivity to steric hindrance on arylboronic acids **1** (e.g. **47c**, Scheme 30), with a dramatic drop in the yield of **38** when going along the aromatic substitution series *para*→*meta*→*ortho* (R^1 = H, R^2 = Cl; 93%, 65% and <5% respectively).

Kobayashi proposes that the mechanism commences by reaction of the aniline **46** and boronic acid substrate **1** with the Cu catalyst **B**, to produce complex **AK** (Scheme 31). Oxidation of complex **AK** by the oxidised photocatalyst $Ir(ppy)_3^+$, (generated from oxidation of the excited state photocatalyst $Ir(ppy)_3^*$ by molecular oxygen), produces Cu(III) complex **AL**. Reductive elimination of complex **AL** releases the coupled product **47** and Cu(I) complex **A**. The active Cu(II) catalyst **B** is then regenerated *via* oxidation by another oxidised photocatalyst. Kobayashi proposes that this oxidation step could also be carried out by singlet oxygen ($^1O_2$) generated by energy transfer from the excited state photocatalyst to molecular oxygen. However, no trace of $^1O_2$ could be found when chemical tests for the excited state oxygen species were carried out.

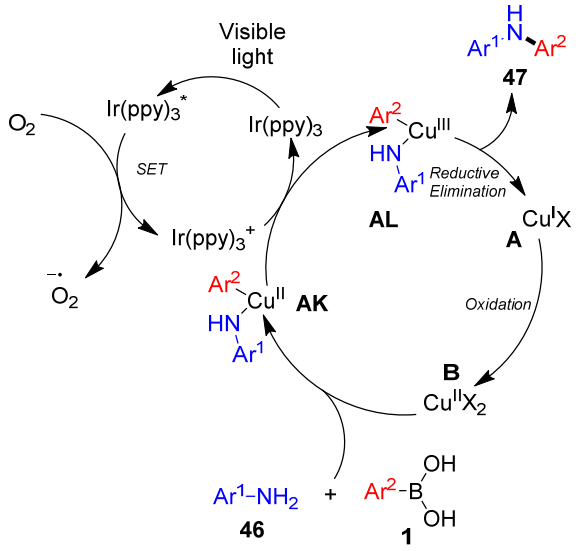

Scheme 31. Mechanism Proposed for photoredox-mediated Chan-Lam coupling by Kobayashi and co-workers.[34]

That same year (2015), Kobayashi also developed a photoredox-mediated Ullmann coupling of carbazoles **48**, shown in Scheme 32.[35] The reaction tolerates a range of electronic variation on the aryl iodide **49**, ranging from electron-withdrawing CF_3 groups (e.g. **50b**) to electron-donating OMe (e.g. **50a**) with moderate to good yields (51-79%). Unfortunately, reactive functional groups (such as carbonyl, nitrile and hydroxyl) are not well tolerated and give the products **50** in low yields (<20%). The reaction was also shown to be relatively insensitive to sterics, with no significant reduction in yield when changing from using *m*-tolyl iodide to *o*-tolyl iodide as a coupling partner (73% *vs*. 68%). The reaction is also tolerant of heteroaromatic iodides (54-93%, e.g. **50c**, Scheme 32) and various alkyl, aryl and halogen substituents on the carbazole ring **48** (e.g. **50d**, Scheme 32).

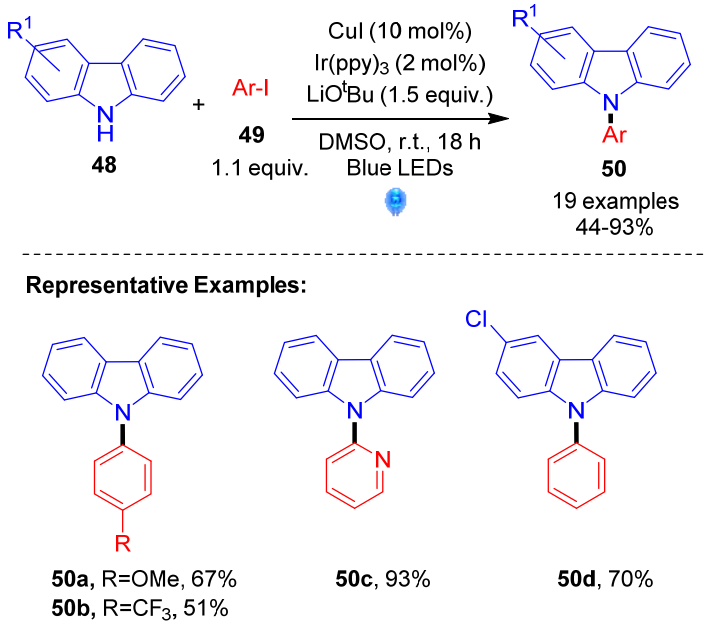

Scheme 32. Photoredox-mediated Ullmann coupling developed by Kobayashi and co-workers.[35]

Kobayashi's proposed mechanism begins with two successive additions of carbazole **48** to copper iodide, giving complex **AN** (Scheme 33). At this point, in contrast to most dual copper- and photoredox-catalytic reactions, the photocatalyst is not thought to affect the copper complex by single electron transfer. Instead, the excited state photocatalyst $Ir(ppy)_3^*$ quenches itself by transferring its excess energy to **AN**, generating excited state copper complex **AN***. This excited state complex then reduces aryl iodide **49** *via* a single electron transfer, generating complex **AO** and an aryl radical **AP**. These two species subsequently interact, releasing the product **50** and regenerating the active copper complex **AM**. The main evidence for this mechanism comes from the fact that the excited state photocatalyst $Ir(ppy)_3$ does not have sufficient oxidative potential to oxidise copper complex **AN** ($E_{1/2}^{*III/II}$ = -0.3 V *vs*. Fc/Fc^+). Additionally, fluorescence quenching experiments demonstrate that the excited state photocatalyst cannot be quenched by the aryl iodide **49**. Nevertheless, the mechanism proposed in Scheme 33 is only an assumed one until further mechanistic evidence is gathered.

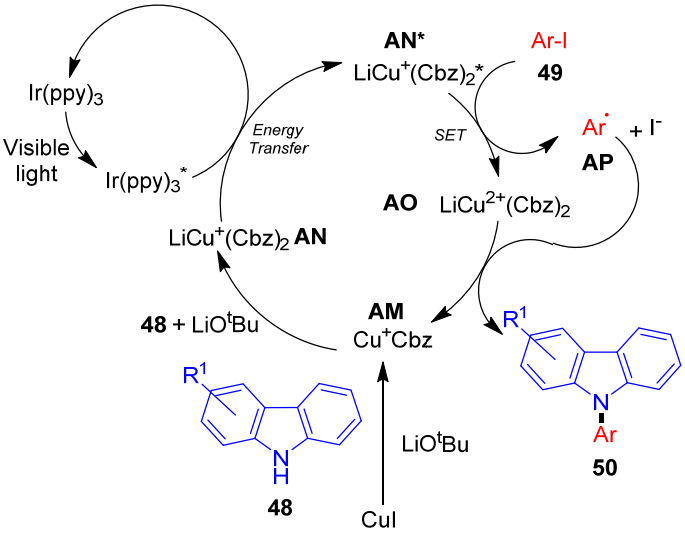

Scheme 33. Mechanism proposed by Kobayashi and co-workers.[35]

Recently, Liu and co-workers have demonstrated that dual copper- and photoredox-catalysis is compatible not only with preformed photocatalysts, that we have seen in many of the examples discussed so far, but also with photocatalysts which are formed *in situ*. In 2017, Liu reported a protocol for the synthesis of aminothiazoles **52** catalysed by a $Cu(NCS)_2^-$ catalyst produced *in situ* which acts both as a photocatalyst and as a Lewis acid catalyst (Scheme 34).[36]

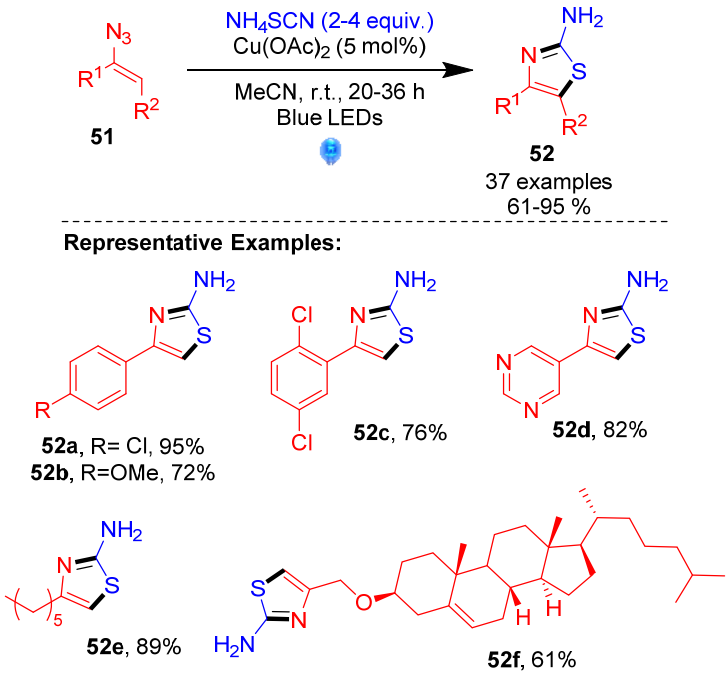

Scheme 34. Dual copper- and photoredox-catalysed synthesis of aminothiazoles developed by Liu and co-workers.[36]

The conditions developed by Liu allowed for a wide scope of both aryl and alkyl vinyl azides **51** to be converted to the corresponding aminothiazole **52** in good to excellent yields (61-95%). Aryl azides bearing electron withdrawing groups on the aromatic ring prove to be excellent substrates, furnishing the products **52** in excellent yields (95% for **52a**). In contrast substrates with electron donating substituents on the aromatic ring give slightly reduced yields (e.g. 72% of **52b**). The reaction is also tolerant of sterically demanding aryl azides, yielding the products in good yields (e.g. 76% for **52c**). Heteroaryl vinyl azides also prove to be excellent substrates, furnishing the desired products in good yields (e.g. 82% for **52d**). In addition to (hetero)aryl vinyl azides, alkyl vinyl azides are also highly compatible substrates for this transformation, providing products **52** in good to excellent yields (e.g. **52e**, 89%), including a number of products which contain potentially reactive groups such as amines, esters and alkynes. This is another dual copper- and photoredox-protocol which has shown itself to be of potential use in a pharmaceutical chemistry setting, as Liu and co-workers were able to use this methodology to prepare an aminothiazole analogue of cholesterol in good yield (**52f**, 61%). This potential is further highlighted by the authors who implemented the protocol as part of a number of synthetic sequences in order to synthesize a range of biologically active compounds. The authors also conducted a number of mechanistic experiments in order ascertain the mechanism of the reaction (Scheme 35).

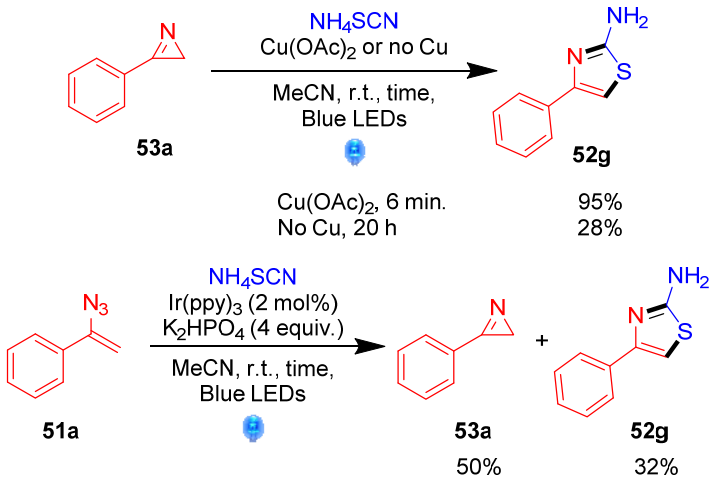

Scheme 35. Mechanistic experiments carried out by Liu and co-workers.[36]

When azirdine **53a** was exposed to the reaction conditions, product **52g** could be obtained in high yield (95%). In the absence of the copper catalyst, this yield was significantly reduced (28%). It was also shown that under photoredox conditions, aryl vinyl azide **51a** could be converted to aziridine **53a**, with aminothiazole **52g** formed as a minor product. The results of these experiments indicated that aziridine **53** was an intermediate in the catalytic cycle, which results in formation of the final product **52**. These results also show that this intermediate is most likely formed through a photoredox-catalysed energy transfer process of vinyl azide **51**. In addition to this evidence, it was also shown that mixing $Cu(OAc)_2$ and NH_4SCN results in a species which exhibits a strong absorption maximum between 350 and 560 nm. Mass spectrometry analysis of this mixture revealed a peak corresponding to $Cu(NCS)_2^-$ which is thought to be the photocatalytic species generated *in situ*. Quenching experiments also show that the addition of vinyl azide **51a** quenches the chemiluminescence of the photocatalyst formed. Based on these mechanistic investigations, Liu and co-workers propose the mechanism shown in Scheme 36.

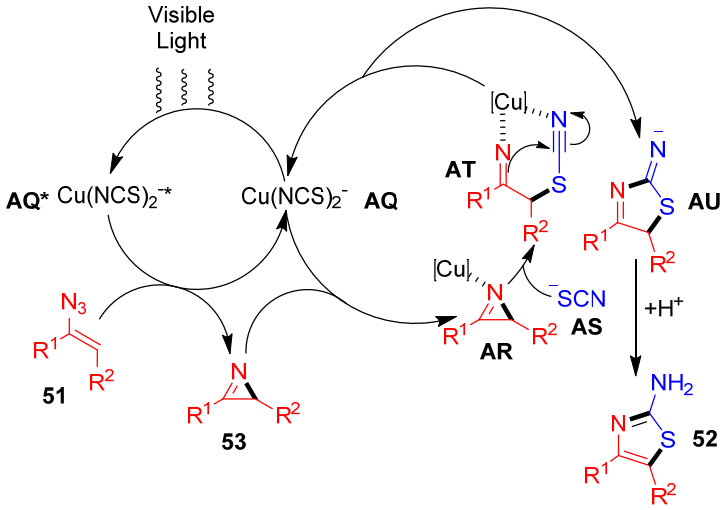

Scheme 36. Mechanism proposed by Liu and co-workers.[36]

The authors propose that the transformation begins by photoexcitation of copper catalyst **AQ**, formed from the mixture of $Cu(OAc)_2$ and NH_4SCN, to give excited state complex **AQ***. Energy transfer from **AQ*** to substrate **51** regenerates ground state **AQ** and ultimately results in cyclisation of **51** to give aziridine **53**.

Co-ordination of the copper catalyst **AQ** to the aziridine **53** gives intermediate **AR**, which is then subject to a nucleophilic ring opening by the thiocyanide anion **AS**, which gives chelated intermediate **AT**. Cyclisation of this intermediate releases copper catalyst **AQ** and intermediate **AU**, which after addition of a proton can then tautomerise to product **52**.

The next reaction by Peters and Fu, involves a catalytic system where it is thought that the photoredox catalyst and the cross-coupling species are formed *in situ* from the same initial copper reagent (Scheme 37).[37]

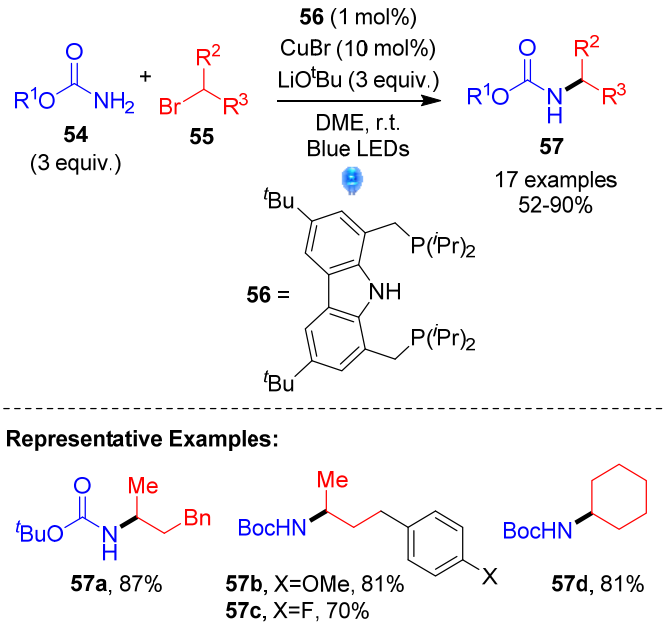

Scheme 37. Cross-coupling of amides and alkyl bromides reported by Peters and Fu.[37]

This transformation expands the scope of nitrogen coupling partners to carbamates **54** and secondary unactivated alkyl bromides **55** in a formal nucleophilic substitution reaction. Interestingly, the authors report that traditional ruthenium and iridium photocatalysts, which are normally used for dual catalysis, are incompatible with this reaction. Prior to the development of the *in situ* photocatalyst formation protocol, Peters, Fu and co-workers first investigated the formation and photophysical properties of the photoactive catalyst. Through these studies they were able to identify that the copper photocatalyst **58** formed is ligated with ligand **56** (Figure 1).

Having isolated complex **58**, the authors were then able to characterise the photophysical properties of the complex and also demonstrate that it is able to catalyse the reaction when added directly to the reaction mixture as a discrete complex. With the properties of the photoactive copper complex and its catalytic activity confirmed, Peters and Fu and co-workers then set about ascertaining the substrate scope for this transformation. The reaction was shown to tolerate a range of steric bulk on the carbamate **54** substituent (with R^2 = Me, R^3 = CH_2Bn), ranging from methyl (90%) to *tert*-butyl (**57a**, 87%). There was a slight drop in yield when chains ending in aryl or silyl groups were used (67% and 76% respectively). Cyclic carbamates were also compatible in the reaction (74%). In terms of the secondary alkyl bromide **55**, substituent chains which end in aryl substituents with electron-donating (**57b**, 81%) and electron-withdrawing (**57c**, 70%) both make for good substrates. R alkyl groups containing silyl ethers perform well (72%), however, the yield of the reaction suffers if R alkyl groups containing aryl ethers are present (56%) (R^2 = Me in **54**, R^1 = ^{t}Bu in **55**). Cyclic alkyl bromides proved to be excellent substrates, with ring sizes varying from 6-8 furnishing the desired products **57** in excellent yields (81-88%, e.g. **57d**). Curiously, when cyclopentyl bromide is employed in the reaction, the yield decreases dramatically (49%); this result was improved by switching to a Hg lamp as the light source, increasing the yield to 74% (**54** R^1 = ^{t}Bu).

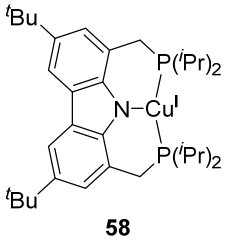

Figure 1. Photoactive complex isolated by Peters, Fu and co-workers.[37]

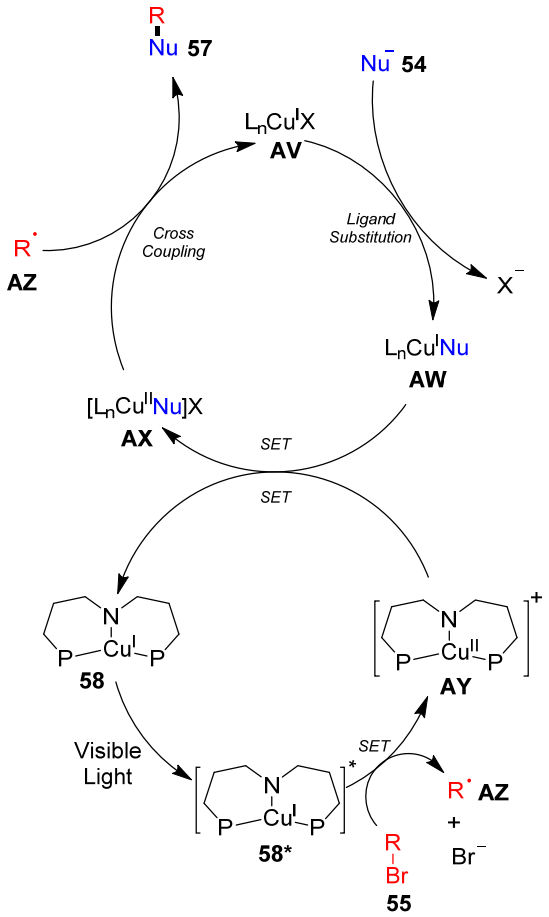

Scheme 38. Mechanism proposed by Peters and Fu.[37]

Included in this work is a proposed mechanism for this transformation, based on synergistic catalysis by two different copper complexes (Scheme 38). Peters and Fu postulate that the transformation begins with a base mediated ligand substitution of the carbamate nucleophile onto complex **AV** to produce intermediate **AW**. Meanwhile, visible light excitation of photocatalyst **58** and subsequent single electron transfer from **58*** promotes reduction of alkyl bromide **55** to form alkyl radical **AZ**. This reduction also results in oxidation of the excited state copper photocatalyst **58***, giving oxidised species **AY**. Oxidised copper species **AY** in turn oxidises copper complex **AW** by means of a second single electron transfer, to yield Cu(II) complex **AX** while

also regenerating ground state complex **58** in the process. Cross-coupling with the previously generated alkyl radical **AZ** releases alkylated product **57**. Although the authors do not detail what this cross-coupling step entails, it most likely goes through sequential radical addition to generate a Cu(III) intermediate followed by reductive elimination to release the product **57** and regenerate the catalytically active Cu(I) complex **AV**.

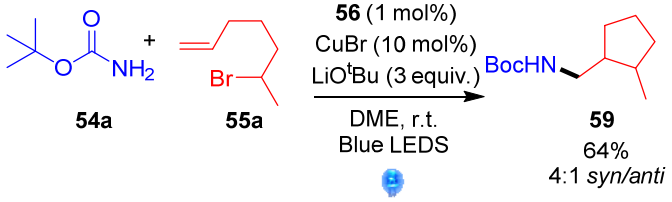

Scheme 39. Mechanistic reaction carried out by Peters and Fu and co-workers.[37]

In support of this mechanism, the authors present several mechanistic studies, with the primary evidence being the selectivity of an intramolecular cyclisation carried out under their standard conditions (Scheme 39). Fu and co-workers report that the *syn/anti* selectivity of the reaction shown in Scheme 39 indicates that it is proceeding through a radical mechanism, citing that similar radical based cyclisations give the same selectivity.[38] Additional data to support this mechanism includes the observation of a signal in the EPR spectrum of the reaction mixture, which is consistent with species **AX**. However, it is unclear at this stage whether the reaction occurs *via* an inner sphere SET, similar to the work of Reiser discussed previously,[12] or an outer sphere SET. In a similar vein, Peters and Fu have also reported an elegant asymmetric copper-catalysed C-N cross coupling, where the copper is both the photocatalyst as well as source of asymmetric induction, however, further mechanistic studies will be required to shed light on the exact mechanistic details of this reaction.[6a]

3.2. C-O and C-S Bond Formation

Compared with C-N bond forming reactions, examples of other C-heteroatom bond forming reactions that use dual copper- and photoredox-methodology in the literature are much scarcer. To date there has only been one reported example of a dual copper- and photoredox-catalysed C-O bond forming reaction. This reaction was reported by Nicewicz in 2017, as part of their research into halolactonisations (Scheme 40).[39] Remarkably, the dual catalytic system comprising acridinium photocatalyst **28** and copper co-catalyst shown in Scheme 40 was found to provide the opposite regioselectivity compared to classical halolactonisations.

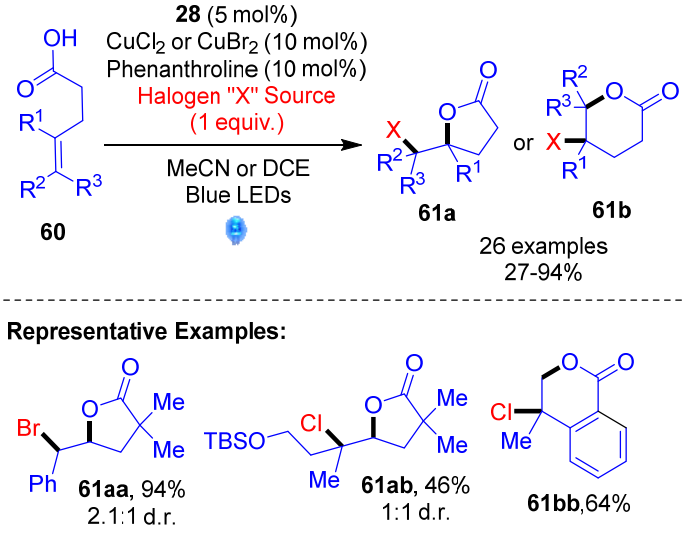

Scheme 40. Halolactonisation protocol developed by Nicewicz and co-workers.[39]

Using this protocol, Nicewicz and co-workers synthesised a range of chlorinated and brominated lactones **61a** or **61b** (identity of product formed depending on substitution pattern on **60**), by tailoring the halogen source to the substrate used. For chlorofunctionalisation reactions, the authors used either *N*-chlorosuccinimide (NCS) or *N*-chlorophthalimide (NCP), whereas for the bromofunctionalisations the authors used diethyl bromomalonate (DEBM) or *N*-bromophthalimide (NBP) as the halogen source. Under these conditions, a range of styrenes with different substitution patterns were tolerated in the reaction giving good yields of **61a** (64-94%) with moderate diastereoselectivity (1.3:1 to 2.9:1 d.r.; R^3 = H, R^1 = H, Me; e.g. **61aa**, Scheme 40). Notably, styrenes with electron donating groups (e.g. OMe) on the aromatic ring were incompatible with the bromination protocol due to the instability of the benzyl bromide intermediates. The reaction was also applicable for tri-substituted aliphatic alkenes including those with silyl ether protecting groups (e.g. **61ab**, 46%). Benzoic acid substrates **60** are also compatible, giving the product **61bb** in reasonable yield (64%).

The carboxylic acid nucleophile in **60** can also be replaced with alcohols or protected amines to yield the corresponding cyclised products in moderate to good yields (57-71%). The reaction protocol can also be utilised for intermolecular reactions but with reduced yields (27-59%). As part of this work, Nicewicz and his group proposed a mechanism for the halolactonisation reaction which is shown in Scheme 41.

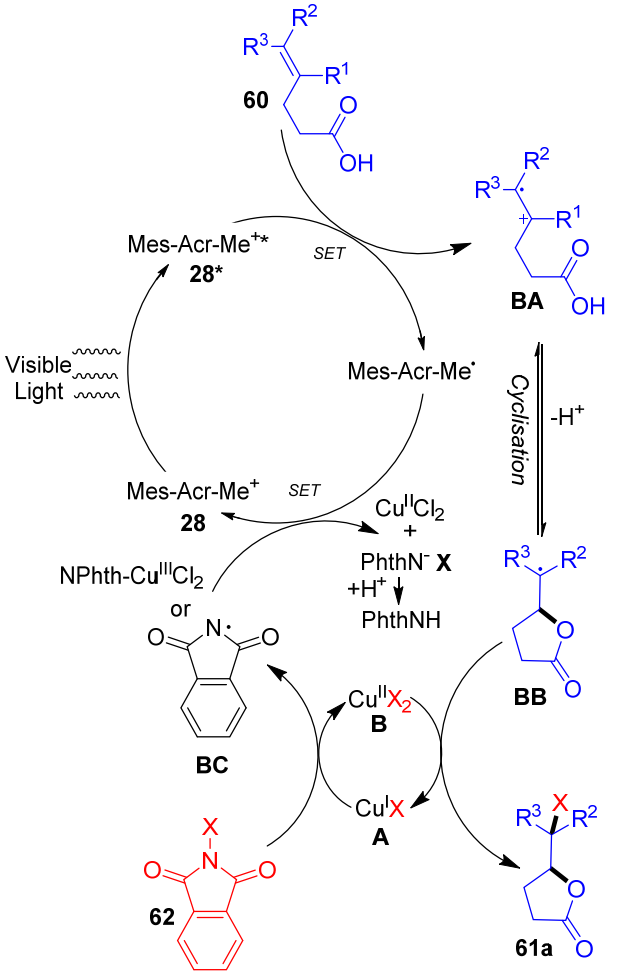

Scheme 41. Halolactonisation mechanism proposed by Nicewicz and co-workers.[39]

The mechanism proposed by Nicewicz begins with the single electron oxidation of the substrate **60** by the excited state acridinium dye **28***, generating radical cation **BA**. This radical cation subsequently cyclises with the loss of a proton to give **BB**, which then obtains a halogen from copper catalyst **B** to yield product **61a**. The authors suggest that the intervening steps require further study, but could feasibly proceed *via* the copper catalyst and photocatalyst being regenerated by the external halogen source. First Cu complex **A** is oxidised by the halogen source **62** to regenerate **B** and produce a phthalimide radical **BC**. The ground state photocatalyst **28** is then regenerated by a single electron oxidation of the reduced catalyst Mes-Acr-Mes· by the phthalimide radical **BC**, or by a Cu^{III} species. There are a number of pieces of evidence to support the proposed mechanism. Firstly, UV/vis experiments carried out by Nicewicz and his group established that NCP **62** is capable of oxidising **A** to **B**. In addition, the phthalimide by-product that would expected if this was the mechanism is indeed observable by both ^{1}H NMR and GC-MS analysis. The reduction potential of the phthalimide radical **BC** is also high enough that it can feasibly regenerate the photocatalyst by single electron transfer. Nevertheless, the authors do state that further investigation is required to conclusively prove other steps in the mechanism.

As with C-O bond forming reactions, there has been only one C-S dual copper- and photoredox-catalysed bond forming reaction reported in the literature to date. This report emerged from Yang, Wu and co-workers in 2017.[40] In this work, they reveal a protocol for the C4-H sulfonylation of 1-napthylamides **63** using sodium sulfinates **64**; key to the selectivity of this reaction is the use of a picolinamide directing group (Scheme 42). Yang, Wu and co-workers also report that these transformations can be performed using a dual copper and silver co-catalysis strategy, but for the purpose of this review only the dual copper- and photoredox-methodology will be discussed.

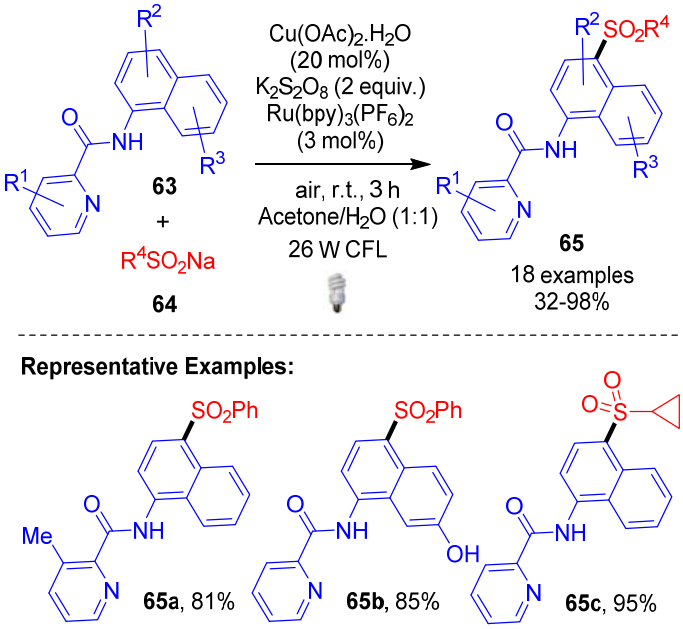

Scheme 42. Sulfonylation protocol developed by Yang and Wu.[40]

The reaction described in Scheme 42 shows a reasonable amount of steric tolerance for substrate **63**, as a methyl group can be tolerated in the *ortho* position of the pyridine ring (**65a**, 81%). However, when the pyridine of the directing group in **63** is substituted for an isoquinoline ring, the authors report a lower yield (62%) which they reason is due to steric clashes. A range of electron-withdrawing and -donating groups are tolerated on the naphthalene ring in **63**, furnishing products **65** in moderate to good yields (55%-93%; R^4 = Ph). Notably, these included highly reactive functional groups such as hydroxyl (**65b**) and bromide groups. Sodium sulfinates **64** with mildly electron-poor or -rich aryl substituents were reported to be excellent substrates (91%-93%; (R^1, R^2 and R^3 = H). In contrast, when a strongly electron-withdrawing substituent was installed on the aryl ring (R^4 on **64**), the yield of the coupled products **65** dropped dramatically (40%-45%). Sodium sulfinates bearing alkyl substituents also performed well in the reaction giving the products **65c** in excellent yield (95%). Unfortunately sterically demanding aryl substituents such as napthyl were not tolerated under the copper photoredox methodology and heteroaromatic sodium sulfinates performed poorly (31%). The synthetic utility of this transformation is further improved by the reaction being amenable to scale up to gram scale synthesis. This allowed the reaction to be carried out on a 5 mmol scale with no appreciable drop in reaction performance (91%; R^1, R^2 and R^3 = H, R^4 = Ph). Furthermore, the authors report facile hydrolysis of products **65** under alkaline conditions to provide access to biologically relevant 4-sulphonylnaphylamine scaffolds.

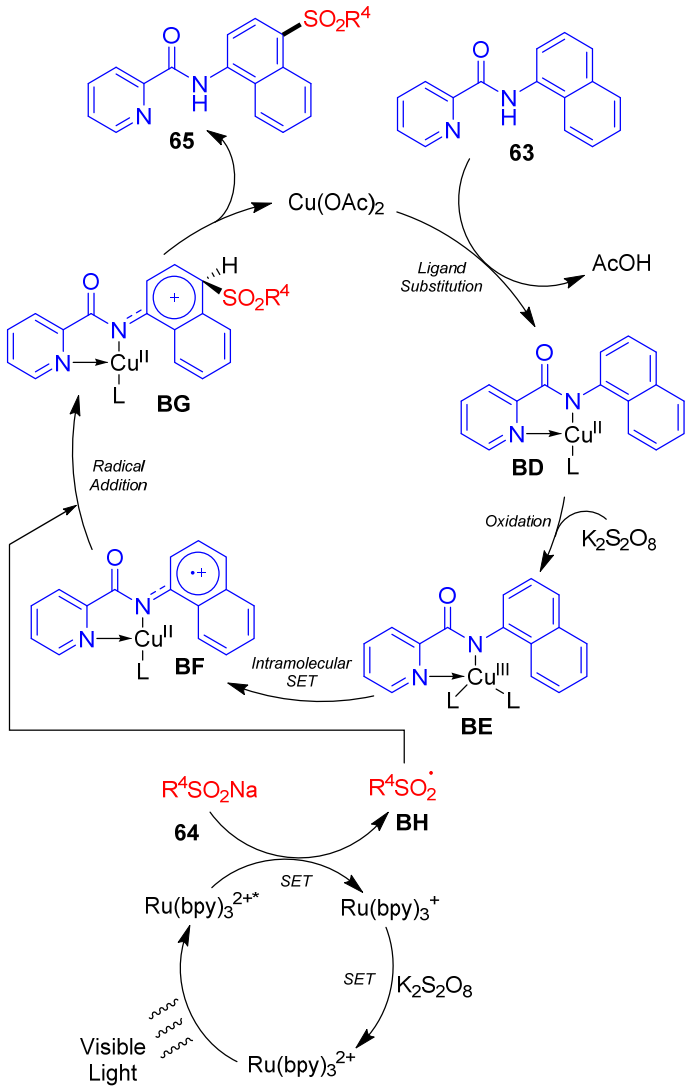

Scheme 43. Mechanism for the C-H sulfonylation experiment proposed by Yang and Wu.[40]

The mechanism proposed by Yang, Wu and co-workers suggests that bidentate chelation of the substrate **63** to the catalyst is key for the observed reactivity (Scheme 43). Thus, the proposed mechanism begins with ligand substitution of substrate **63** onto the copper acetate catalyst, generating chelated complex **BD**. The copper centre in complex **BD** can then be oxidised by $K_2S_2O_8$ to give Cu(III) intermediate **BE**. It is then proposed that this intermediate undergoes a single electron oxidation of the ligand by the metal centre to generate the radical cation ligand in complex **BF**. Meanwhile, the sodium sulfinate salt **64** can undergo single electron oxidation by photoexcited $Ru(bpy)_3^{2+*}$ to generate a sulfonyl radical **BH** and reduced $Ru(bpy)_3^{+}$, from which the ground state photocatalyst is regenerated by a single electron oxidation from $K_2S_2O_8$. The sulfonyl radical **BH** can then react with the radical cation ligand in **BF** to produce species **BG**. Proton transfer followed by ligand displacement of species **BG** by acetate releases product **65** and regenerates the active copper catalyst. The authors present several pieces of evidence to support their mechanistic hypothesis. Firstly, many of the reactions studied benefited from the inclusion of NaOPiv as a base. Yang and Wu reason that this benefit stems from the base helping to deprotonate the amide nitrogen in **63**, allowing the substrate to chelate onto the copper catalyst more effectively. Additionally, substrates where the directing group in **63** is removed or the amide nitrogen is substituted or not present, do not participate in the reaction at all, further supporting the idea that this reaction requires bidentate chelation of the substrate to the copper catalyst. The authors also varied the atmosphere under which the reactions were carried out and observed no difference in yield between the reactions under air and under nitrogen indicating that oxidation by molecular oxygen is not occurring in the mechanism. Radical trapping experiments using butylated hydroxytoluene (BHT) not only inhibited the reaction but also produced the sulfonyl-BHT adduct (detected by HR-MS), indicating that the mechanism of the transformation is radical based and involves **BH**.

Nevertheless, it should be noted that the mechanism proposed in Scheme 43 is only a putative one until further mechanistic proof is established.

3.3. C-X π-Bond Forming Reactions

To date there have only been a couple of examples of dual copper- and photoredox-catalysed oxidation reactions.

The first example, reported by Cheng in 2015 is the *tert*-butyl hydroxyperoxide (TBHP) mediated oxidation of *N*-2-alkynylphenyl α-amino carbonyl compounds **66** to oxalic amides **67** using photoredox catalysis (Scheme 44).[41] Although the mechanism is not currently clear for this process, the authors do suggest that the photoredox cycle oxidises **66** to the corresponding imine, and that the role of copper is as a Lewis acid to activate this imine intermediate towards oxidation by TBHP. The reaction is tolerant of a range of aryl and alkyl substituents R^2 and Me, F or Cl are tolerated at R^1 on **66** (Scheme 44). However, yields were generally moderate (32-69%) due to a competing hydrolysis reaction.

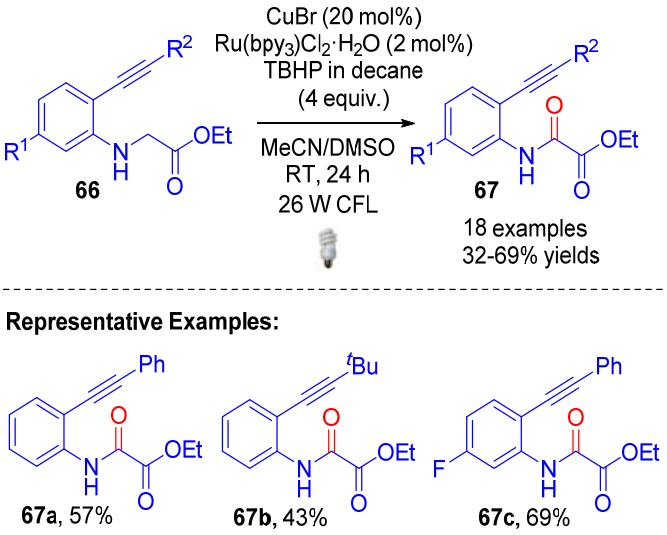

Scheme 44. TBHP-mediated aerobic oxidation of N-2-alkynylphenyl α-amino carbonyl compounds developed by Cheng and co-workers.[41]

The second example of dual copper- and photoredox-catalysed oxidation was reported in 2017 by Tao.[42] In this work, Tao and his group document their development of a dual catalytic protocol for the aerobic oxidation of amines **68** to nitriles **69** (Scheme 45).

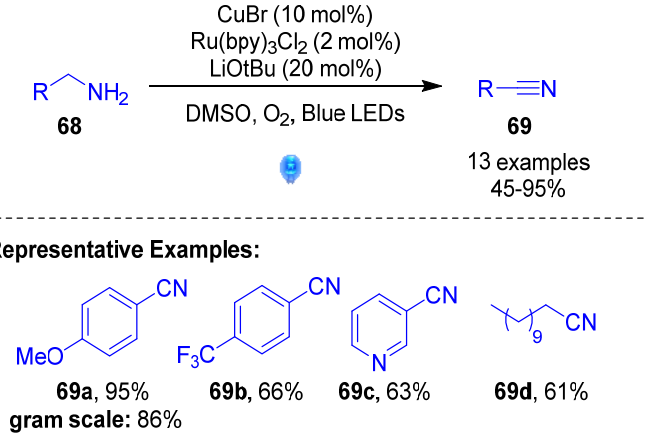

Scheme 45. Dual copper- and photoredox-catalysed aerobic oxidation of amines developed by Tao and co-workers.[42]

Using this protocol, they were able to oxidise a wide range of amines **68** in moderate to excellent yields. When oxidising benzylamines, electron-rich amines perform better than electron-poor amines (77-95% *vs.*45-66%, e.g. **69a** *vs.* **69b**). Benzylamines with aromatics which are traditionally sterically demanding such as those with *ortho* substituents are well tolerated in the reaction and make excellent substrates (73%-93%). In addition, heterocyclic benzylic amines are also compatible substrates, with benzylic amines derived from pyridine and thiophene furnishing the desired products **69** in slightly reduced yields of 63% (**69c**) and 50% respectively. The authors also reported that the amine scope could be extended to aliphatic amines with the use of extended reaction times (36 h *vs.* 18 h for aryl amines), giving alkyl nitriles **69** in good yields (e.g. **69d**, 61%). Tao and co-workers also demonstrate that their reaction is easily scalable to gram scale (10 mmol), providing **69a** in 86% yield with photocatalyst loadings as low as 0.5 mol%. The authors acknowledge that an in-depth mechanistic study will be required to elucidate the mechanism of this oxidation reaction. Nevertheless, they do propose a plausible mechanism for the dual copper- and photoredox-catalysed oxidation of amines (Scheme 46).

The proposed mechanism begins with addition of amine substrate **68** to copper catalyst **A** to generate intermediate **BI**. Reductive quenching of $Ru(bpy)_3^{2+*}$ by copper-amide complex **BI** then generates the radical cation in **BJ** and $Ru(bpy)_3^{+}$. The photocatalyst $Ru(bpy)^{2+}$ is subsequently regenerated by reduction of molecular oxygen to give a superoxide radical anion ($^{\cdot-}O_2$) which then abstracts a hydrogen from **BJ** to give intermediate **BK**. The resulting hydrogen peroxide anion then deprotonates **BK** to give intermediate **BL**. The two sequential steps of oxidation by the photocatalyst followed by superoxide hydrogen abstraction repeat, giving intermediate **BN**. Dissociation of the nitrile then releases product **69** and regenerates copper catalyst **A**.

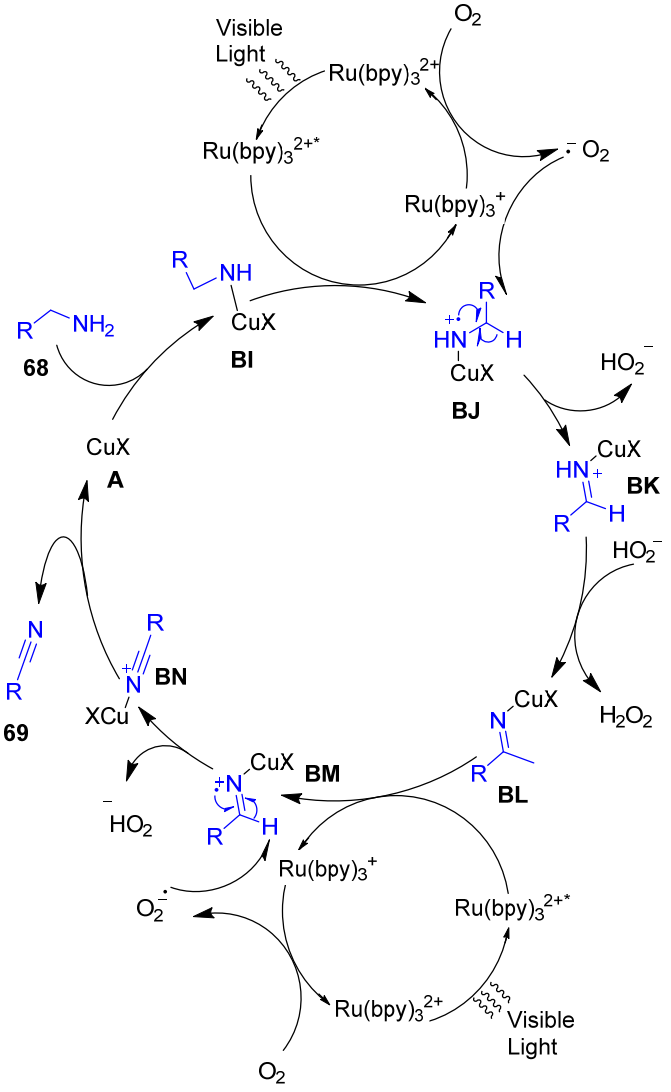

Scheme 46. Dual copper- and photoredox-catalysed oxidation mechanism proposed by Tao.[42]

Until recently, there had been no dual copper- and photoredox-catalysed protocol for the formation of C-C π-bonds. This changed very recently when Glorius and co-workers published a protocol for the decarboxylative olefination of NHP esters **36** in 2018 (Scheme 47).[43] Using these conditions, Glorius and co-workers were able to convert a range of NHP esters **36** to the corresponding alkenes **71** in low to excellent yields, under mild conditions. This protocol is an improvement on previous decarboxylative olefination reactions, which often relied on both harsh reaction conditions (>110 °C) and high-cost catalysts,[44] or enzymes which display poor chemical stability.[45] This reaction also marked the first published example of radical decarboxylation of a redox active NHP ester (**36**) catalysed by an organophotocatalyst (**70**). As mentioned previously, organophotocatalysts are often far cheaper than the transition metal based alternatives. Glorius' conditions are tolerant of a vast range of primary NHP esters **36** with varying structures and functionalities. The reaction was also shown to be an excellent route to allylic substituted aromatics, providing methyl eugenol **71a** and an indole derivative **71b** in good yields (80% and 73% respectively). Under other decarboxylative olefination conditions, these products proved difficult to isolate as they were prone to isomerisation under harsh conditions. Cyclic olefins such as **71c** can also be obtained in high yields (66-94%) from the corresponding secondary NHP ester **36**.

The authors noted that when an acyclic secondary NHP esters **36** ($R^1 = CH_2Bn$, $R^2 = Me$) a 1:1.7 mixture of the terminal and internal alkenes was obtained in excellent yield (>99%). These conditions were also applied to a range of NHP derivatised drug molecules such as chlorambucil, mycophenolic acid and gemfibrozil, furnishing the corresponding alkenes **71** in good to excellent yields (62-87%; e.g. **71d**), thereby highlighting the potential applications of this protocol in late stage drug modification. NHP esters **36** of long chain fatty acids derived from biomass feed stocks (such as oleic acid) also proved to be excellent substrates, furnishing the desired alkene products, such as **71e**, in high yield (88-93%). Glorius and co-workers also performed an additive-based robustness screen, which demonstrated no noticeable decrease in reaction performance in the presence of a number of potentially sensitive functional groups such as nitrile, carbonyl, alkene, acetal, bromobenzene, alkyne and (hetero)aromatics.

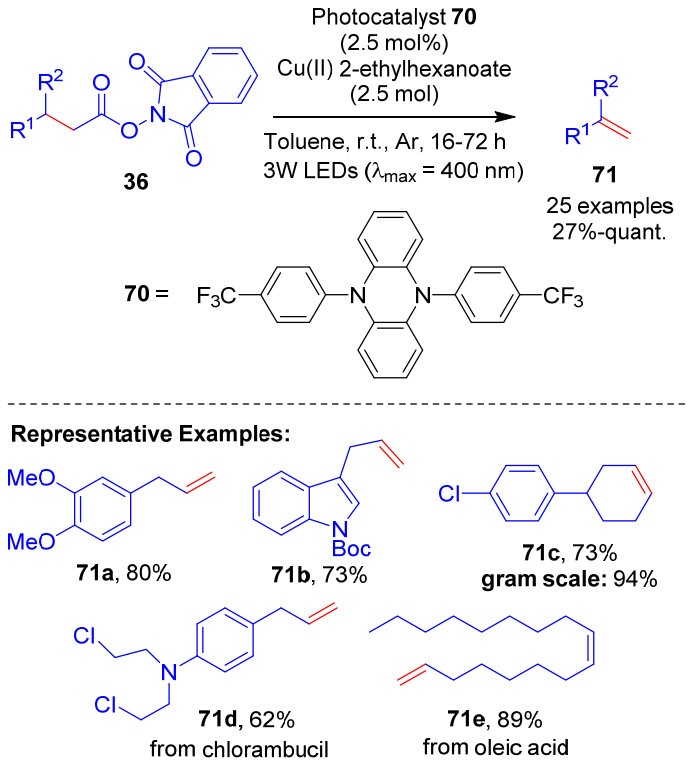

Scheme 47. Decarboxylative olefination reaction developed by Glorius.[43]

A radical clock experiment using substrate **36** where R^1 = cyclopropenyl and R^2 = H resulted in isolation of a 59% yield of 1,3-butadiene, which strongly supports that the decarboxylation mechanism is radical in nature. Further mechanistic studies also show that olefination of the alkyl radical does not occur *via* single electron oxidation from the Cu(II) catalyst, followed by deprotonation, as the expected carbocation intermediate could not be trapped by inclusion of a nucleophile such as ethanol. Kinetics experiments show that the rate equation is zero order in both photocatalyst **70** and NHP ester **36**, indicating that neither of these species are rate limiting. The kinetic data actually suggests that the rate limiting step is the generation of excited state photocatalyst **70*** (Scheme 48), as the reaction exhibits a linear relationship between the reaction rate and the photon flux on the system.

Using the data from these in-depth mechanistic studies, Glorius proposes that the olefination reaction proceeds *via* the mechanism shown in Scheme 48. The proposed mechanism begins with a single electron reduction of substrate **36** by excited state photocatalyst **70***, resulting in decarboxylation, the generation of radical **BR** and a phthaliminde anion **X**. Addition of radical **BR** onto copper catalyst **BO** produces Cu(III) intermediate **BP**. Subsequent reaction of intermediate **BP** and anion **X** yields alkene product **71** and produces copper complex **BQ**. The ground state photocatalyst **70** is then regenerated by single electron transfer from copper complex **BQ**, which regenerates copper catalyst **BO** in the process.

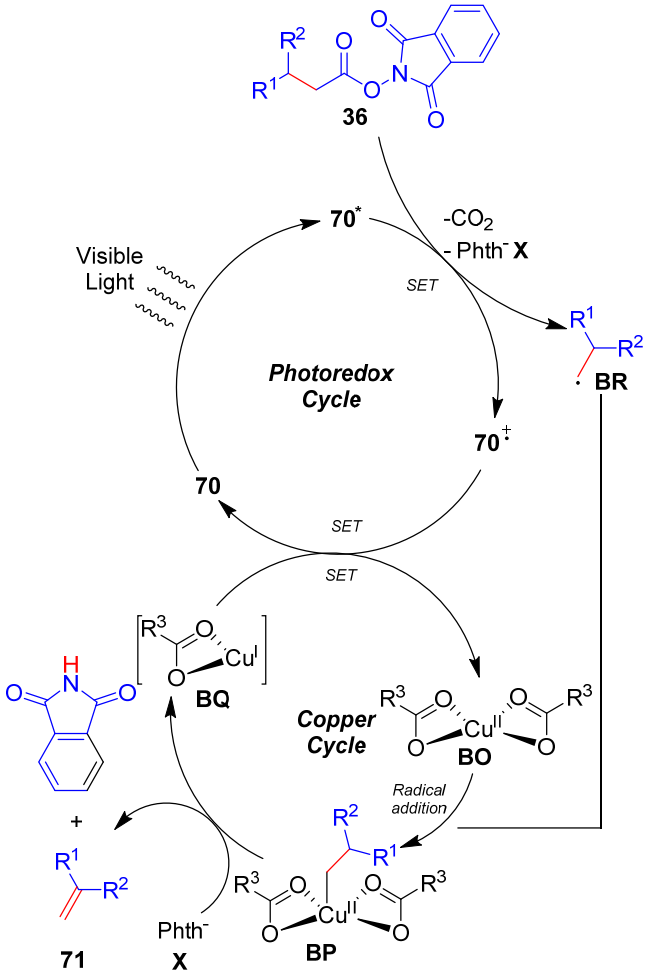

Scheme 48. Mechanism for decarboxylative olefinations proposed by Glorius.[43]

4. Click Chemistry

There have been a number of interesting applications of dual copper- and photoredox-catalysis in copper azide-alkyne cyclisation (CuAAC) click chemistry. In fact, the first ever example of a dual copper- and photoredox-catalysed reaction was a CuAAC reaction reported by Ritter and Konig in 2006,[46] which pre-dates the recent explosion of interest in visible light mediated photoredox-catalysis. In this work, Ritter and Konig used the dual catalytic system in a biomimetic photoreceptor-signal amplification and transduction pathway. In this case, the photocatalyst (riboflavin) acts as a photoreceptor which only becomes active in response to the stimulus of visible light. In the presence of light and a sacrificial reductant (NEt_3) the photocatalyst is able to reduce a Cu(II) source to a Cu(I) source, which is then in the correct oxidation state to catalyse the CuAAC reaction (Scheme 49). Thus, a light stimulus could be amplified and converted into a photochemical output. Other similar biomimetic applications include the work of Devaraj and co-workers, who used a similar CuAAC system to construct a

phospholipid membrane that self-assembled when exposed to visible light.[47] They achieved this by tethering phosphate groups and alkyl chains to the alkyne and azide coupling partners.

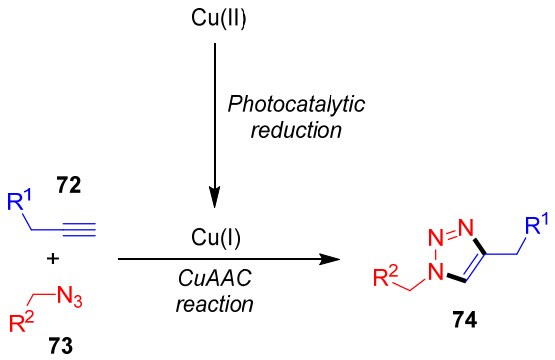

Scheme 49. General reaction pathway for dual copper- and photoredox-catalysed CuAAC reactions.

Other work in this area has focused on the use of these click reactions in synthetic chemistry, with the group of Singh reporting the synthesis of substituted triazoles *via* trapping of cationic intermediates generated by photoredox catalysis with sodium azide followed by a CuAAC click reaction.[48] Dual copper- and photoredox-catalysed CuAAC click reactions have also been developed using heterogenous catalysis, by Duan and co-workers in 2017.[49] Therein, the authors report a heterogenous CuAAC click reaction catalysed by a Cu(II) co-ordination polymer with photoactive linkers. Duan and co-workers believe that under visible light irradiation, the photoactive linker can reduce the Cu(II) centres to Cu(I), which is the catalytically active oxidation state for the CuAAC click reaction.

5. Conclusion

Although still in its infancy, the field of dual copper- and photoredox-catalysis holds much promise for the future in terms of the development of novel organic transformations. It has a number of advantages over other methodologies, such as cheap and relatively non-toxic copper catalysts, mild reaction conditions, as well as the possibility of being adapted to asymmetric synthesis through the utilisation of chiral ligands. These advantages will no doubt lead to the discovery of further useful transformations with high synthetic utility as the field continues to develop. We envisage that these developments will include expanding the scope of substrates and radical sources, in order to expand the range of synthetic targets achievable by dual copper- and photoredox-catalysed methodologies.

Addendum

Since the submission of this manuscript, Macmillan and co-workers have published three papers on dual copper- and photoredox-catalysed reactions: decarboxylative trifluoromethylation of aliphatic carboxylic acids,[50a] trifluoromethylation of bromoarenes[50b] and decarboxylative sp^3 C-N coupling.[50c] Chen, Wu and co-workers have published a one-pot photomediated Giese reaction/Friedel-Crafts hydroalkoxylation/oxidative aromatization.[51] Reiser and co-workers have reported visible-light-mediated atom transfer radical addition (ATRA) reactions of perfluoroalkyl iodides with styrenes and phenylacetylenes.[52] Hu and co-workers have published a cross-coupling of alkyl redox-active esters with benzophenone imines.[53] Patil and co-workers have reported a visible-light mediated cross coupling which is also catalytic in both gold and copper.[54] Li, Bao and co-workers have reported a three-component alkyl-fluorination of olefins with fluoride ion.[55]

Acknowledgments

We would like to thank the Engineering and Physical Sciences Research Council, Heriot-Watt University and CRITICAT Centre for Doctoral Training for financial support [Ph.D. studentship to EM; Grant code: EP/L016419/1].

References and notes

1. For selected reviews, see: a) Matsui, J. K.; Lang, S. B.; Heitz, D. R.; Molander, G. A. *ACS Catal.* **2017,** *7*, 2563-2575; b) Goddard, J.-P.; Ollivier, C.; Fensterbank, L. *Acc. Chem. Res.* **2016,** *49*, 1924-1936; c) Nicholls, T. P.; Leonori, D.; Bissember, A. C. *Nat. Prod. Rep.* **2016,** *33*, 1248-1254; d) Romero, N. A.; Nicewicz, D. A. *Chem. Rev.,* **2016,** *116*, 10075-10166; e) Ghosh, I.; Marzo, L.; Das, A.; Shaikh, R.; König, B. *Acc. Chem. Res.* **2016,** *49*, 1566-1577; f) Levin, M. D.; Kim, S.; Toste, F. D. *ACS Cent. Sci.* **2016,** *2*, 293-301; g) Douglas, J. J.; Sevrin, M. J.; Stephenson, C. R. J. *Org. Process Res. Dev.* **2016,** *20*, 1134-1147; h) Shaw, M. H.; Twilton, J.; MacMillan, D. W. C. *J. Org. Chem.* **2016,** *81*, 6898-6926; i) Angnes, R. A.; Li, Z.; Correia, C. R. D.; Hammond, G. B. *Org. Biomol. Chem.* **2015,** *13*, 9152-9167; j) Peña-López, M.; Rosas-Hernández, A.; Beller, M. *Angew. Chem. Int. Ed.* **2015,** *54*, 5006-5008; k) Nicewicz, D. A.; Nguyen, T. M. *ACS Catal.* **2014,** *4*, 355-360; l) Schultz, D. M.; Yoon, T. P. *Science* **2014,** *343*, 1239176; m) Prier, C. K.; Rankic, D. A.; MacMillan, D. W. C. *Chem. Rev.* **2013,** *113*, 5322-5363; n) Zou, Y.-Q.; Chen, J.-R.; Xiao, W.-J. *Angew. Chem. Int. Ed.* **2013,** *52*, 11701-11703; o) Xi, Y.; Yi, H.; Lei, A. *Org. Biomol. Chem.* **2013,** *11*, 2387-2403; p) Reckenthäler, M.; Griesbeck, A. G. *Adv. Synth. Catal.* **2013,** *355*, 2727-2744; q) Xuan, J.; Xiao, W.-J. *Angew. Chem. Int. Ed.* **2012,** *51*, 6828-6838; r) Tucker, J. W.; Stephenson, C. R. J. *J. Org. Chem.* **2012,** *77*, 1617-1622; s) Narayanam, J. M. R.; Stephenson, C. R. J. *Chem. Soc. Rev.* **2011,** *40*, 102-113.
2. For selected reviews, see: a) Twilton, J.; Le, C.; Zhang, P.; Shaw, M. H.; Evans, R. W.; MacMillan, D. W. C. *Nat. Rev. Chem.* **2017,** *1*, 0052; b) Lang, X.; Zhao, J.; Chen, X. *Chem. Soc. Rev.* **2016,** *45*, 3026-3038; c) Hoffmann, N. *ChemCatChem* **2015,** *7*, 393-394; d) Hopkinson, M. N.; Sahoo, B.; Li, J.-L.; Glorius, F. *Chem. Eur. J.* **2014,** *20*, 3874-3886.
3. For selected reviews, see: a) Cavalcanti, L. N.; Molander, G. A. *Top. Curr. Chem.* **2016,** *374*, 39; b) Gui, Y.-Y.; Sun, L.; Lu, Z.-P.; Yu, D.-G. *Org. Chem. Front.* **2016,** *3*, 522-526; c) Tellis, J. C.; Kelly, C. B.; Primer, D. N.; Jouffroy, M.; Patel, N. R.; Molander, G. A. *Acc. Chem. Res.* **2016,** *49*, 1429-1439; d) Vila, C. *ChemCatChem* **2015,** *7*, 1790-1793; e) Gutierrez, O.; Tellis, J. C.; Primer, D. N.; Molander, G. A.; Kozlowski, M. C. *J. Am. Chem. Soc.* **2015,** *137*, 4896-4899; f) Tellis, J. C.; Primer, D. N.; Molander, G. A. *Science* **2014,** *345*, 433; g) Zuo, Z.; Ahneman, D. T.; Chu, L.; Terrett, J. A.; Doyle, A. G.; MacMillan, D. W. C. *Science* **2014,** *345*, 437.
4. For example, nickel(II) chloride ethylene glycol dimethyl ether complex and bis(1,5-cyclooctadiene)nickel(0) are known carcinogens.
5. Ye, Y.; Sanford, M. S. *J. Am. Chem. Soc.* **2012,** *134*, 9034-9037.
6. For selected examples, see: a) Kainz, Q. M.; Matier, C. D.; Bartoszewicz, A.; Zultanski, S. L.; Peters, J. C.; Fu, G. C. *Science* **2016,** *351*, 681; b) Sagadevan, A.; Hwang, K. C. *Adv. Synth. Catal.* **2012,** *354*, 3421-3427; c) Creutz, S. E.; Lotito, K. J.; Fu, G. C.; Peters, J. C. *Science* **2012,** *338*, 647;

For selected examples where UV is used instead of visible light, see: d) Ahn, J. M.; Ratani, T. S.; Hannoun, K. I.; Fu, G. C.; Peters, J. C. *J. Am. Chem. Soc.* **2017,** *139*, 12716-12723; e) Ratani, T. S.; Bachman, S.; Fu, G. C.; Peters, J. C. *J. Am. Chem. Soc.* **2015,** *137*, 13902-13907; f) Do, H.-Q.; Bachman, S.; Bissember, A. C.; Peters, J. C.; Fu, G. C. *J. Am. Chem. Soc.* **2014,** *136*, 2162-2167; g) Tan, Y.; Munoz-Molina, J. M.; Fu, G. C.; Peters, J. C. *Chem. Sci.* **2014,** *5*, 2831-2835; h) Uyeda, C.; Tan, Y.; Fu, G. C.; Peters, J. C. *J. Am. Chem. Soc.* **2013,** *135*, 9548-9552; i) Ziegler, D. T.; Choi, J.; Muñoz-Molina, J. M.; Bissember, A. C.; Peters, J. C.; Fu, G. C. *J. Am. Chem. Soc.* **2013,** *135*, 13107-13112; j) Bissember, A. C.; Lundgren, R. J.; Creutz, S. E.; Peters, J. C.; Fu, G. C. *Angew. Chem. Int. Ed.* **2013,** *52*, 5129-5133.

7. For selected examples, see: a) Parasram, M.; Gevorgyan, V. *Chem. Soc. Rev.* **2017,** *46*, 6227-6240; b) Pirtsch, M.; Paria, S.; Matsuno, T.; Isobe, H.; Reiser, O. *Chem. Eur. J.* **2012,** *18*, 7336-7340.
8. For selected reviews, see: a) Larsen Christopher, B.; Wenger Oliver, S. *Chem. Eur. J.* **2017,** *24*, 2039-2058; b) Hernandez-Perez, A. C.; Collins, S. K. *Acc. Chem. Res.* **2016,** *49*, 1557-1565; c) Reiser, O. *Acc. Chem. Res.* **2016,** *49*, 1990-1996; d) Paria, S.; Reiser, O. *ChemCatChem* **2014,** *6*, 2477-2483.
9. Müller, K.; Faeh, C.; Diederich, F. *Science* **2007,** *317*, 1881.
10. a) Wang, X.; Truesdale, L.; Yu, J.-Q. *J. Am. Chem. Soc.* **2010,** *132*, 3648-3649; b) Cho, E. J.; Senecal, T. D.; Kinzel, T.; Zhang, Y.; Watson, D. A.; Buchwald, S. L. *Science* **2010,** *328*, 1679.
11. Cismesia, M. A.; Yoon, T. P. *Chem. Sci.* **2015,** *6*, 5426-5434.
12. Bagal Dattatraya, B.; Kachkovskyi, G.; Knorn, M.; Rawner, T.; Bhanage Bhalchandra, M.; Reiser, O. *Angew. Chem. Int. Ed.* **2015,** *54*, 6999-7002.
13. Saveant, J.-M. In *Advances in Physical Organic Chemistry;* Bethel, D. Ed.; Academic Press, 1990; pp. 115-129.
14. Rawner, T.; Knorn, M.; Lutsker, E.; Hossain, A.; Reiser, O. *J. Org. Chem* **2016,** *81*, 7139-7147.
15. Lin, Q.-Y.; Ran, Y.; Xu, X.-H.; Qing, F.-L. *Org. Lett.* **2016,** *18*, 2419-2422.
16. a) Rewcastle, G. W.; Gamage, S. A.; Flanagan, J. U.; Frederick, R.; Denny, W. A.; Baguley, B. C.; Kestell, P.; Singh, R.; Kendall, J. D.; Marshall, E. S.; Lill, C. L.; Lee, W.-J.; Kolekar, S.; Buchanan, C. M.; Jamieson, S. M. F.; Shepherd, P. R. *J. Med. Chem.* **2011,** *54*, 7105-7126; b) Smart, B. E. *Chem. Rev.* **1996,** *96*, 1555-1556.
17. Zhang, H.-R.; Chen, D.-Q.; Han, Y.-P.; Qiu, Y.-F.; Jin, D.-P.; Liu, X.-Y. *Chem. Commun.* **2016,** *52*, 11827-11830.
18. a) Ruiz Espelt, L.; Wiensch, E. M.; Yoon, T. P. *J. Org. Chem.* **2013,** *78*, 4107-4114; b) Freeman, D. B.; Furst, L.; Condie, A. G.; Stephenson, C. R. J. *Org. Lett.* **2012,** *14*, 94-97; c) Bock, C. R.; Connor, J. A.; Gutierrez, A. R.; Meyer, T. J.; Whitten, D. G.; Sullivan, B. P.; Nagle, J. K. *J. Am. Chem. Soc.* **1979,** *101*, 4815-4824.
19. Rueping, M.; Koenigs, R. M.; Poscharny, K.; Fabry, D. C.; Leonori, D.; Vila, C. *Chem. Eur. J.* **2012,** *18*, 5170-5174.
20. Perepichka, I.; Kundu, S.; Hearne, Z.; Li, C.-J. *Org. Biomol. Chem.* **2015,** *13*, 447-451.
21. Li, Z.; Li, C.-J. *Org. Lett.* **2004,** *6*, 4997-4999.
22. Shi, D.; He, C.; Qi, B.; Chen, C.; Niu, J.; Duan, C. *Chem. Sci.* **2015,** *6*, 1035-1042.
23. Querard, P.; Perepichka, I.; Zysman-Colman, E.; Li, C.-J. *Beilstein J. Org. Chem.* **2016,** *12*, 2636-2643.
24. Yang, F.; Koeller, J.; Ackermann, L. *Angew. Chem. Int. Ed.* **2016,** *55*, 4759-4762.
25. Zhang, H.; Zhang, P.; Jiang, M.; Yang, H.; Fu, H. *Org. Lett.* **2017,** *19*, 1016-1019.
26. a) Ke, J.; Tang, Y.; Yi, H.; Li, Y.; Cheng, Y.; Liu, C.; Lei, A. *Angew. Chem. Int. Ed.* **2015,** *54*, 6604-6607; b) Alberti, A.; Macciantelli, D.*;* Brustolon, M.; Giamello, E. Eds.; John Wiley & Sons, Inc.: Hoboken, NJ, 2009; pp. 287-323.
27. Xia, X.-F.; Zhang, G.-W.; Wang, D.; Zhu, S.-L. *J. Org. Chem.* **2017,** *82*, 8455-8463.
28. a) Fukuzumi, S.; Ohkubo, K.; Suenobu, T. *Acc. Chem. Res.* **2014,** *47*, 1455-1464; b) Fukuzumi, S.; Kotani, H.; Ohkubo, K.; Ogo, S.; Tkachenko, N. V.; Lemmetyinen, H. *J. Am. Chem. Soc.* **2004,** *126*, 1600-1601; c) Fukuzumi, S.; Ohkubo, K. *Org. Biomol. Chem.* **2014,** *12*, 6059-6071.
29. Wang, D.; Zhu, N.; Chen, P.; Lin, Z.; Liu, G. *J. Am. Chem. Soc.* **2017,** *139*, 15632-15635.
30. Flamigni, L.; Barbieri, A.; Sabatini, C.; Ventura, B.; Barigelletti, F. In *Photochemistry and Photophysics of Coordination Compounds II;* Balzani, V.; Campagna, S. Eds.; Springer Berlin Heidelberg: Berlin, Heidelberg, 2007; pp. 143-203.
31. Jin, R.; Chen, Y.; Liu, W.; Xu, D.; Li, Y.; Ding, A.; Guo, H. *Chemical Communications* **2016,** *52*, 9909-9912.
32. Hsieh, S.-Y.; Bode, J. W. *ACS Central Science* **2017,** *3*, 66-72.
33. Xiang, M.; Meng, Q. Y.; Li, J. X.; Zheng, Y. W.; Ye, C.; Li, Z. J.; Chen, B.; Tung, C. H.; Wu, L. Z. *Chem. Eur. J.* **2015,** *21*, 18080-18084.
34. Yoo, W.-J.; Tsukamoto, T.; Kobayashi, S. *Angew. Chem. Int. Ed.* **2015,** *54*, 6587-6590.
35. Yoo, W.-J.; Tsukamoto, T.; Kobayashi, S. *Org. Lett.* **2015,** *17*, 3640-3642.
36. Lei, W.-L.; Wang, T.; Feng, K.-W.; Wu, L.-Z.; Liu, Q. *ACS Catal.* **2017,** *7*, 7941-7945.
37. Ahn, J. M.; Peters, J. C.; Fu, G. C. *J. Am. Chem. Soc.* **2017,** *139*, 18101-18106.
38. Lusztyuk, J. M., B.; Deycard, S.; Lindsay, D. A.; Ingold, K. U. *J. Org. Chem.* **1987,** *52*, 3509-3514.
39. Griffin, J. D.; Cavanaugh, C. L.; Nicewicz, D. A. *Angew. Chem. Int. Ed.* **2017,** *56*, 2097-2100.
40. Bai, P.; Sun, S.; Li, Z.; Qiao, H.; Su, X.; Yang, F.; Wu, Y.; Wu, Y. *J. Org. Chem.* **2017,** *82*, 12119-12127.
41. Liu, W.; Liu, S.; Xie, H.; Qing, Z.; Zeng, J.; Cheng, P. *RSC Advances* **2015,** *5*, 17383-17388.
42. Tao, C.; Wang, B.; Sun, L.; Liu, Z.; Zhai, Y.; Zhang, X.; Wang, J. *Org. Biomol. Chem.* **2017,** *15*, 328-332.
43. Tlahuext-Aca, A.; Candish, L.; Garza-Sanchez, R. A.; Glorius, F. *ACS Catal.* **2018,** *8*, 1715-1719.
44. a) Chatterjee, A.; Hopen Eliasson, S. H.; Törnroos, K. W.; Jensen, V. R. *ACS Catal.* **2016,** *6*, 7784-7789; b) Liu, Y.; Kim, K. E.; Herbert, M. B.; Fedorov, A.; Grubbs, R. H.; Stoltz, B. M. *Adv. Synth. Catal.* **2014,** *356*, 130-136; c) Maetani, S.; Fukuyama, T.; Suzuki, N.; Ishihara, D.; Ryu, I. *Organometallics* **2011,** *30*, 1389-1394; d) Miller, J. A.; Nelson, J. A.; Byrne, M. P. *J. Org. Chem* **1993,** *58*, 18-20.
45. a) Grant, J. L.; Hsieh, C. H.; Makris, T. M. *J. Am. Chem. Soc.* **2015,** *137*, 4940-4943; b) Dennig, A.; Kuhn, M.; Tassoti, S.; Thiessenhusen, A.; Gilch, S.; Bülter, T.; Haas, T.; Hall, M.; Faber, K. *Angew. Chem. Int. Ed.* **2015,** *54*, 8819-8822.
46. Ritter, S. C.; Konig, B. *Chem. Commun.* **2006**, 4694-4696.
47. Hardy, M. D.; Konetski, D.; Bowman, C. N.; Devaraj, N. K. *Org. Biomol. Chem.* **2016,** *14*, 5555-5558.
48. Mishra, A.; Rai, P.; Srivastava, M.; Tripathi, B. P.; Yadav, S.; Singh, J.; Singh, J. *Catal. Lett.* **2017,** *147*, 2600-2611.
49. Guo, X.; Zeng, L.; Wang, Z.; Zhang, T.; He, C.; Duan, C. *RSC Adv.* **2017,** *7*, 52907-52913.
50. a) Kautzky, J. A.; Wang, T.; Evans, R. W.; MacMillan, D. W. C. *J. Am. Chem. Soc.* **2018,** *140*, 6522-6526; b) Le, C.; Chen, T. Q.; Liang, T.; Zhang, P.; MacMillan, D. W. C. *Science* **2018,** *360*, 1010-1014; c) Liang, Y.; Zhang, X.; MacMillan, D. W. C. *Nature* **2018**, *559*, 83-88.
51. Liu, H.; Ma, L.; Zhou, R.; Chen, X.; Fang, W.; Wu, J. *ACS Catal.* **2018,** *8*, 6224-6229.

52. Rawner, T.; Lutsker, E.; Kaiser, C. A.; Reiser, O. *ACS Catal.* **2018,** *8*, 3950-3956.
53. Mao, R.; Balon, J.; Hu, X. *Angew. Chem. Int. Ed.* **2018,** *57*, 9501-9504.
54. Chakrabarty, I.; Akram, M. O.; Biswas, S.; Patil, N. T. *Chem. Commun.* **2018,** *54*, 7223-7226.
55. Deng, W.; Feng, W; Li, Y; Bao, H. *Org. Lett.* **2018**, *20*, 4245-4249.